

Project Title: Solar Resource GIS Data Base for the Pacific Northwest using Satellite Data

Final Report

Report period—October 1, 2000 through December 31, 2003

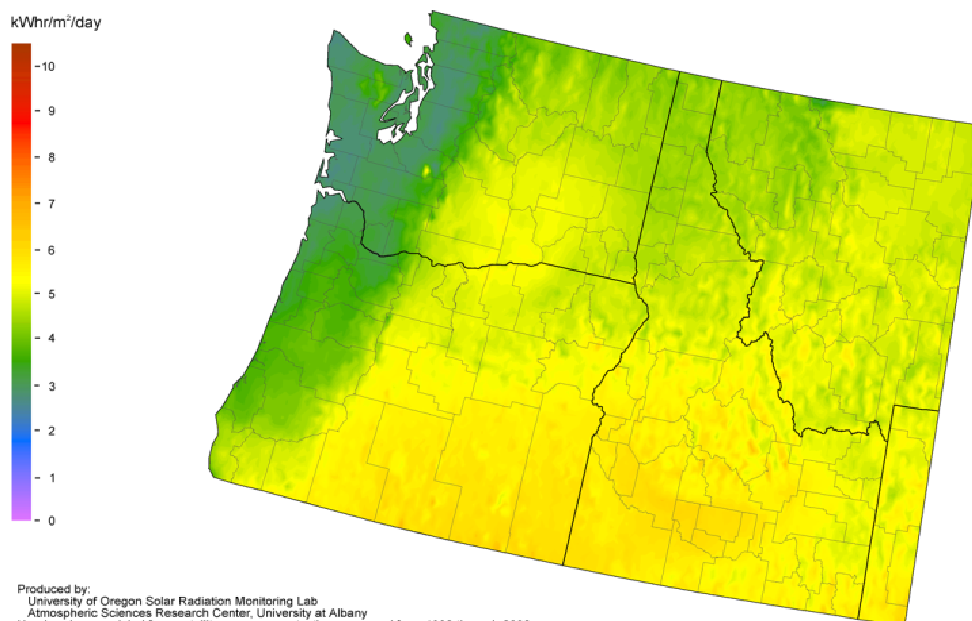
Prepared by: Frank Vignola—UO SRML  
Richard Perez—ASRC

March 29, 2004

Project Identification Number: DE-PS36-0036-00GO10499

Submitted by Frank Vignola – UO SRML  
Department of Physics  
1274—University of Oregon  
Eugene, OR 97403-1274  
Richard Perez *et al.* – ASRC  
ASRC, the University of Albany  
251 Fuller Road  
Albany, NY 12203

Direct Normal Solar Radiation - Annual



Produced by:  
University of Oregon Solar Radiation Monitoring Lab  
Atmospheric Sciences Research Center, University at Albany  
Hourly values modeled from satellite measurements, then averaged from 1998 through 2002  
<http://solardata.uoregon.edu>  
(C) 2004

## Disclaimer

This report was prepared as an account of work sponsored by an agency of the United States Government. Neither the United States Government nor any agency thereof, nor any of their employees, makes any warranty, express or implied, or assumes any legal liability or responsibility for the accuracy, completeness, or usefulness of any information, apparatus, product, or process disclosed, or represents that its use would not infringe privately owned rights. Reference herein to any specific commercial product, process, or service by trade name, trademark, manufacturer, or otherwise does not necessarily constitute or imply its endorsement, recommendation, or favoring by the United States Government or any agency thereof. The views and opinions of authors expressed herein do not necessarily state or reflect those of the United States Government or any agency thereof.

## Abstract

A five year solar radiation database derived from satellite cloud cover and auxiliary data has been created for the Pacific Northwest. The database provides hourly global, beam, and diffuse irradiance values from 1998 through 2002 from longitude  $-110.05^{\circ}$  to  $-125.05^{\circ}$  and north latitude  $42.05^{\circ}$  to  $49.05^{\circ}$  on a  $0.1^{\circ}$  grid. This final report describes the how the database was created, the characteristics of the database, the software tool developed to facilitate the use of the database, and dissemination of the database.

## Table of Contents

Executive Summary.....	5
I. Introduction .....	6
II. Modeling Satellite Data for the Pacific Northwest Solar Resource GIS Data Base .....	6
II. 1 Introduction .....	6
II. 2 Model Improvement.....	6
II. 3 Model Validation .....	8
II. 4 Data Preparation.....	12
III. Further Validation of the Satellite Derived Data .....	13
IV. Production of Solar Resource Maps.....	18
V. Structure of Database.....	19
VI. Solar Angle and PV Performance Calculator .....	20
VII. Distribution of the Database .....	20
VIII. Conclusions.....	21
Appendix A—Satellite to Irradiance Models.....	23
A. 1 A New Operational Satellite-to-Irradiance Model Description, Validation .....	23
A. 2 Producing Satellite-Derived Irradiances in Complex Arid Terrain .....	42
Appendix B—Solar Calculator Information .....	51

Figures

1. Location of ground validation sites .....	8
2. Satellite-derived (Y-axis) vs. ground measured (X-axis) hourly global irradiance (left) and direct irradiance (right) in Burns, OR. The top two plots represent model validation after implementation of model improvements, while the bottom two plots pertain to the model as it was at the beginning of the project. ....	9
3. Same as Fig. 2, but for Hermiston, OR.....	9
4. Same as Fig. 2, but for Eugene, OR.....	10
5. Same as Fig. 2, but for Klamath Falls, OR .....	10
6. Same as Fig. 2, but for Gladstone, OR .....	11
7. Comparing hourly estimates from satellite (Y axis bottom left) and from a neighboring measurement station (Y-axis top right) to ground measurements). The plot at bottom right shows neighboring station estimation error increase as a function of distance. The red horizontal line represents satellite estimation error. ....	11
8. Example of satellite-derived solar resource maps [averaged direct irradiance for the months of February, April, July and November 2000]	
9. Comparison of global irradiance as determined from satellite measurements and from ground based measurements. ....	14
10. Comparison of beam irradiance as determined from satellite measurements and from ground based measurements. ....	14
11. Comparison of diffuse irradiance as determined from satellite measurements and from ground based measurements.....	14
12. Difference between beam irradiance obtained from satellite modeling and ground based measurements. Small blue circles are January, February, and December data points. The red X's are data from the rest of the year. The black line is the trend line.....	15
13. Difference between global irradiance obtained from satellite modeling and ground based measurements. Blue circles January, February, and December. Red Xs rest of year. ....	15
14. Difference between diffuse irradiance obtained from satellite modeling and ground based measurements. Blue circles January, February, and December. Red Xs rest of year. ....	15
15. Comparison of satellite derived global irradiance to ground based measurements against zenith angle. ....	16
16. Comparison of satellite derived beam irradiance to ground based measurements against zenith angle.....	16
17. Comparison of satellite derived diffuse irradiance to ground based measurements against zenith angle. ....	16
18. Plot of difference between satellite derived and ground based measurements of global irradiance plotted against time of day. Red bars represent standard deviation. ....	17
19. Plot of difference between satellite derived and ground based measurements of beam irradiance plotted against time of day. Red bars represent standard deviation.....	17
20. Plot of difference between satellite derived and ground based measurements of diffuse irradiance plotted against time of day. Red bars represent standard deviation. ....	17
21. Change in yearly average beam irradiance from 1978 through 2002 for the three stations that have long-term beam measurements in the UO SRML solar monitoring network.....	18
22. Solar resource map of the annual global irradiance. A map of the annual beam irradiance is shown on the cover of this report .....	19

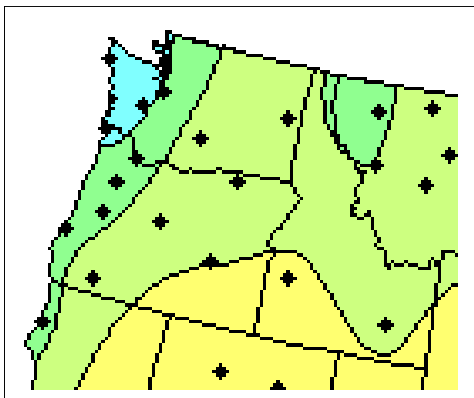
## Executive Summary

A high quality solar radiation database was created for the Pacific Northwest on a 0.1° grid. This is 16 times more detailed than solar resource maps that have been attempted for the region and 100 times more detailed than publicly available satellite derived solar radiation data. A comprehensive description of the regional solar resource has been created by combining this satellite derived database with the site specific regional solar radiation database. In addition to a long-term high quality short time interval database for engineering and climatological studies, the Pacific Northwest now has an extensive hourly solar radiation database that shows how the solar resource varies across and around the numerous climate zones in the region.

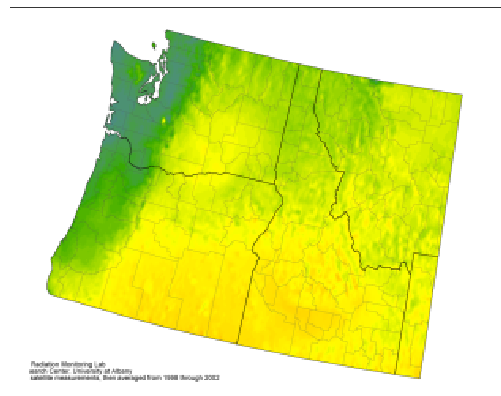
In the process of modeling and testing, improvements have been made to satellite modeling techniques. This has resulted in research papers that have been attached as Appendices A and B.

As the nation expands the use of renewables and invests more in energy efficiency and conservation, the need for a sound solar resource database becomes increasingly important. The utility of the solar radiation database for estimating the performance of passive building technologies, daylighting, and solar electric technologies is obvious. Less easily seen is the usefulness of a comprehensive GIS solar radiation database for conservation and energy efficiency measures. With the database, more accurate and reliable estimates of energy savings can be obtained. The increase in accuracy and reliability of the estimates reduces the uncertainty and risk to the investor and makes it more likely that the measures will be applied. However, it is important that the state energy offices know how to apply the data and that is why it is planned to show how to manipulate the data as well as provide the data. A workshop was held to introduce the state energy offices and utilities in the region about the availability of the new database and to demonstrate the software tool that has been made available to facilitate the use of the database. The data has now been sent to the energy offices of Idaho, Oregon, and Washington along with the software tool to facilitate the use of the data.

Already there are spin-offs from this work as techniques used to develop the solar radiation database will be evaluated for use in updating the National Solar Radiation Data Base and the software tool developed for use of this data is being used to help with the evaluation and siting of rooftop solar electric systems. The climatological and agricultural communities are also showing interest in the database and information about the database has yet to be widely publicized.



*Solar Resource Map as available on the NREL web site*



*Solar resource map produced from the new solar radiation database*

## **I. Introduction**

Over the past three years, the University of Oregon Solar Radiation Monitoring Laboratory (UO SRML) and the Atmospheric Science Research Center of the State University of New York at Albany (ASRC) have been working on gathering satellite, solar radiation, and auxiliary data necessary to produce a detailed solar radiation database for the Pacific Northwest. In addition, work preceded on development a software tool to facilitate the use of the database.

The project is now completed and efforts during this period have resulted in significant improvements in the modeling of global and beam irradiance from satellite data. For this project, 5 years of hourly global, beam, and diffuse solar data on a 0.1° by 0.1° grid have been produced for Idaho, Oregon, and Washington. Data was also produced for western third of Montana and a slice of northwestern Wyoming. A workshop was held in October 2003 for the DOE, state energy offices, and interested utilities on the database and on how to use tools to manipulate the data.

This project has supplied the crucial missing piece in the Pacific Northwest solar resource database. A much clearer picture of the variance of the resource across the region can now be obtained areas with the best solar electric potential can now be identified. Besides the solar industry, we have already seen uses for the data from climatologist, the agricultural community, and those building cell towers in remote locations. This interest resulted from very little publicity and the number of users is expected to increase as the information about the database is made available on the Internet.

In this report, how the database was put together will be discussed along with how the model was tested and verified. Also discussed is the production of maps from the database, software develop to facilitate the use of the database, and distribution of the database and information to the state energy offices in the region.

## **II. Modeling Satellite Data for the Pacific Northwest Solar Resource GIS Data Base**

Prepared by Richard Perez *et al.* ASRC

### **II. 1 Introduction**

The primary objective of our contract was the preparation of solar radiation data set for the Pacific Northwest based upon satellite remote sensing

This objective was to be achieved by:

- (1) Improving and validating the satellite modeling technique against ground truth data.
- (2) Acquiring all necessary input data [including satellite images, snow cover, elevation, climatological turbidity and terrain reflectance characteristics].
- (3) Processing five years of data and creating monthly average maps for the region, along with time/site specific hourly time series for every grid location.

This objective has been achieved successfully and within budget.

## **II. 2 Model Improvement**

The satellite model evolved considerably since the project's onset. While its basic operating principle remains the same – *global irradiance is defined as a quasi linear decreasing function of the relative pixel brightness* – the model became considerably more complex in order to account for the specific conditions found in the northwestern United States. The following modifications were added to the model:

- Creation of a high-resolution monthly climatological gridded turbidity data base. Turbidity is used to define the clearest conditions for the satellite model. Values derived by analyzing pixels at any given month/location cannot exceed clear sky limit for this month/location. Monthly site-specific turbidities were obtained from NREL based upon the data sets they had previously developed for the National Solar Resource Data base (NSRDB).
- Creation of a time-specific gridded snow cover data base. Snow can create problems for the model because its high reflectivity, as seen from the satellite, may be mistakenly interpreted as clouds. Knowing the absence or presence of snow at any location and point in time allows the model to reset its expected darkest possible location-specific pixel value – *defining clear conditions* – to a higher value more representative of new snow. We processed five years of daily high-resolution snow cover reports prepared by the National Operational Hydrological Remote Sensing center branch of NOAA, into an operational model input.
- Creation of terrain reflectance signature data base. The model had been initially developed and tested in the eastern United States, where terrain is generally covered with vegetation. This type of ground cover insures that radiation reflected by the earth's surface and seen by the satellite is distributed isotropically (i.e., no preferential direction of reflectivity). In the western US, vast areas are semi-arid or arid. In these areas the earth acts a little like a mirror when reflecting solar radiation. Reflected radiation is not 100% isotropic but has a specular component. As a result pixel brightness seen by the satellite depends not only on primary solar geometry (the solar zenith angle) but also on the angle between the sun and the satellite's position. Because the amount of specularity varies with ground cover and because ground cover characteristics evolve over the seasons, we had to derive the specular signature of every pixel location representative of every month. This specular signature was derived by analyzing the entire satellite data archive and extracting observed trends for each pixel.
- Implementation of a post model procedure to handle complex terrain situations. Complex terrain is characterized either by extremely bright surfaces, or by the close proximity of bright (highly specular) and dark (isotropic) locations. This type of complexity is often found throughout the Western US. The specular signature data set mentioned above proved to be insufficient to handle the most complex terrain instances and we had to develop an additional correction procedure. The post-modeling procedure consists of a clear sky calibration of model output, and in a few extreme cases the generation of a synthetic data set based upon the removal of mapped singularities.

Details about this development work have been reported in two peer-reviewed publications:

- Perez R., P. Ineichen, K. Moore, M. Kmiecik, C. Chain, R. George and F. Vignola, (2002):

A New Operational Satellite-to-Irradiance Model. *Solar Energy* 73, 5, pp. 307-317

- Perez R., P. Ineichen, M. Kmieciak, K. Moore, R. George and D. Renné, (2003): Producing satellite-derived irradiances in complex arid terrain. Proc. ASES Annual Meeting, Austin, TX. And solar Energy (in press, accepted for publication 12/03)

These two publications are provided in Appendix A.

### **II. 3 Model Validation**

Model output was compared to high quality ground measurements recorded by the University of Oregon in Burns, OR, Hermiston, OR, Eugene, OR, Klamath Falls, OR and Gladstone, OR (see Fig. 1). These sites are representative of the diversity of environments found in the Pacific Northwest region and ranging from temperate maritime

Model validation results are reported in the two articles referenced above and attached in appendix. A summary of these validations is provided in a series of scatter plots comparing ground measured and satellite estimated global and direct irradiances (Figs 2-6). As can be seen, satellite derived irradiances provide an acceptable match to ground observations overall. It is important to note that much of the scatter observed between ground and satellite is inherent to the differences of time and scales between the two measurement methods. Ground measurements are pinpoint locations, whereas satellite pixels are extended in scale (~ 10 x 10 km). The natural spatial variability of cloud fields automatically leads to differences between the two measurement methods except for totally cloudless conditions, hence some of the observed scatter. This point is illustrated in Fig. 7, where the measurements at two ground stations 15 km apart are compared to satellite estimate. The amount of scatter between the two stations, caused by slightly different vantage points, is roughly equivalent to the satellite scatter. This issue had been described in detail in a former publication by the author and colleagues [1].



*Fig. 1 Location of ground validation sites*



Figure 2: Satellite-derived (Y-axis) vs. ground measured (X-axis) hourly global irradiance (left) and direct irradiance (right) in Burns, OR. The top two plots represent model validation after implementation of model improvements, while the bottom two plots pertain to the model as it was at the beginning of the project.

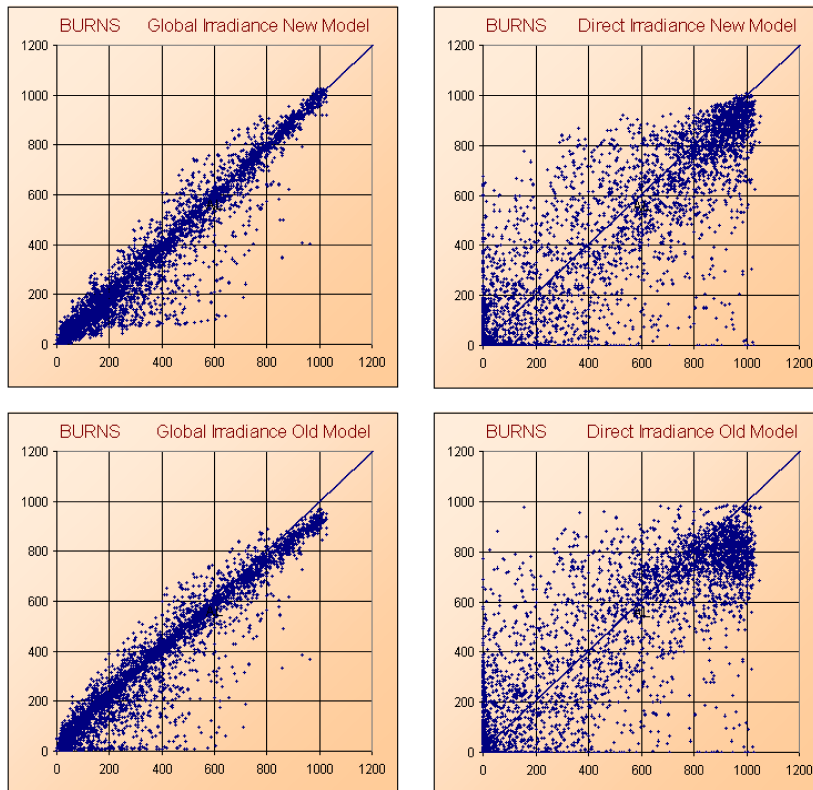


Figure 3: same as Figure 2, but for Hermiston, OR

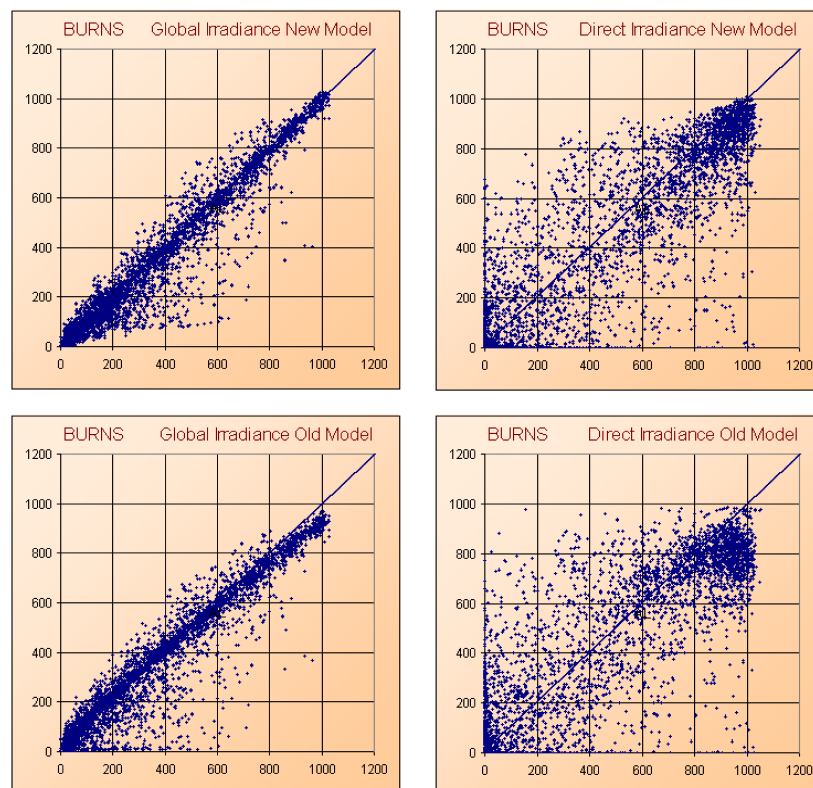


Figure 4: same as Figure 2,  
but for Eugene, OR  
fev@darkwing.uoregon.edu

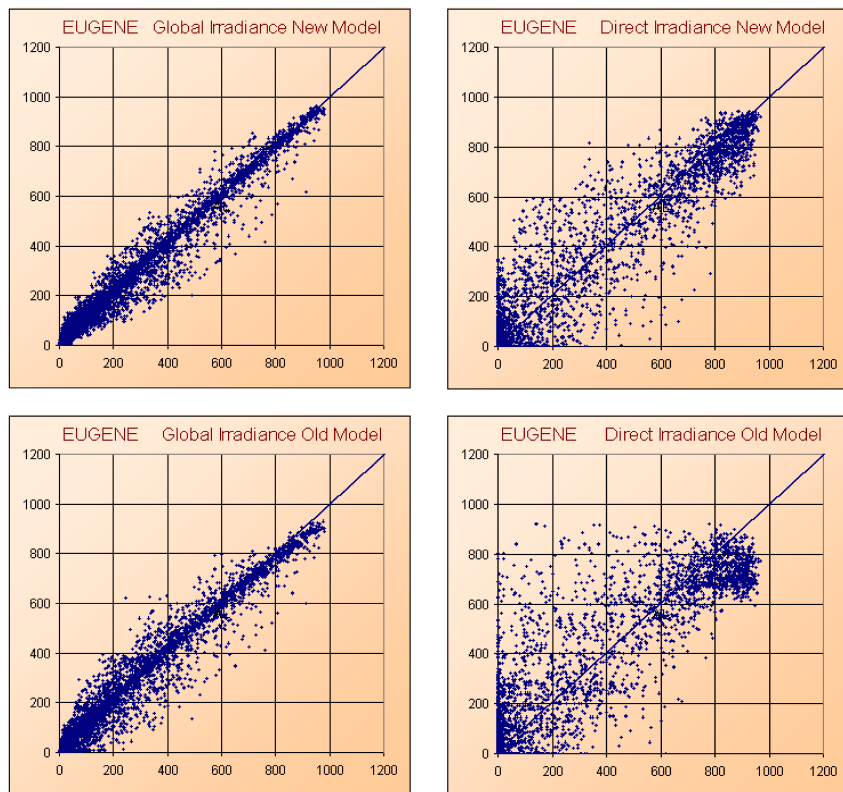


Figure 5: same as Figure 2,  
but for Klamath Falls, OR

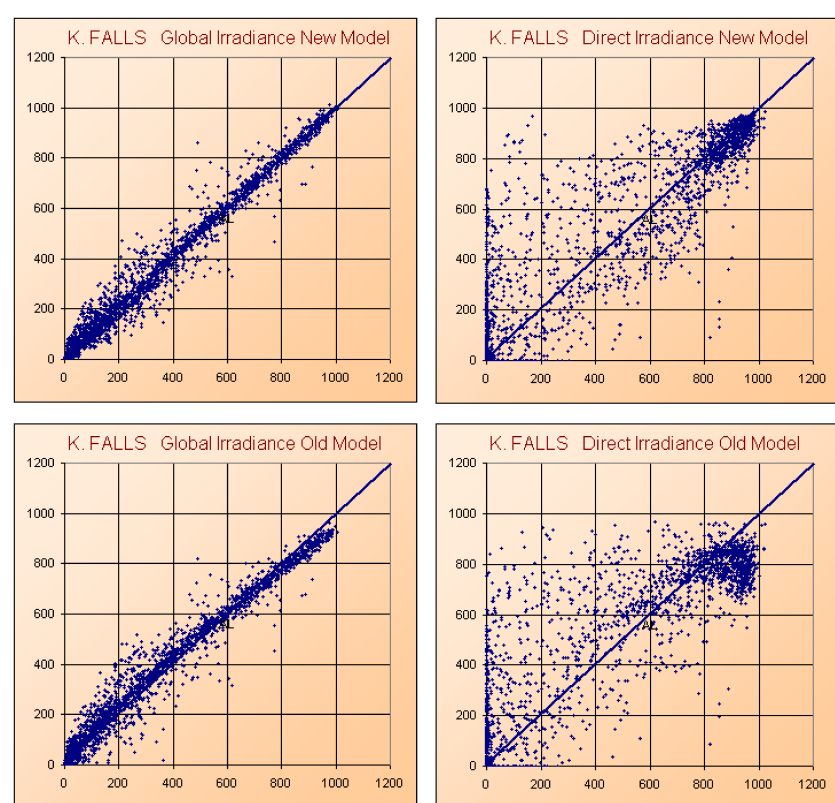


Figure 6: same as Figure 2, but for Gladstone, OR

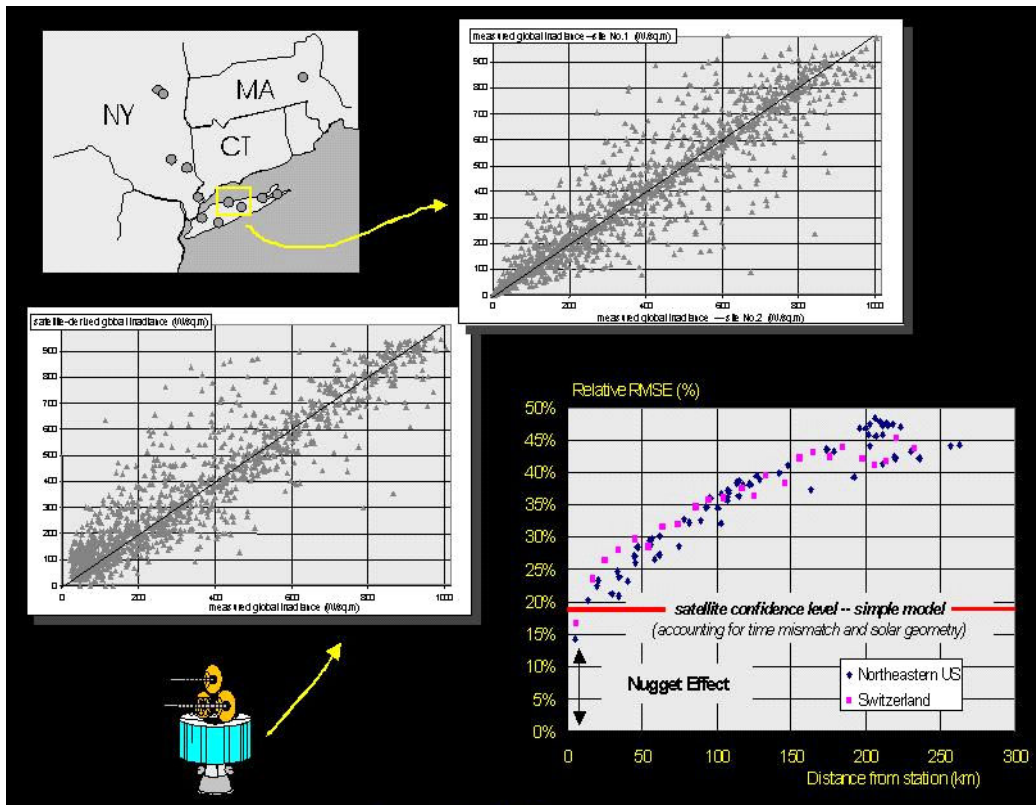
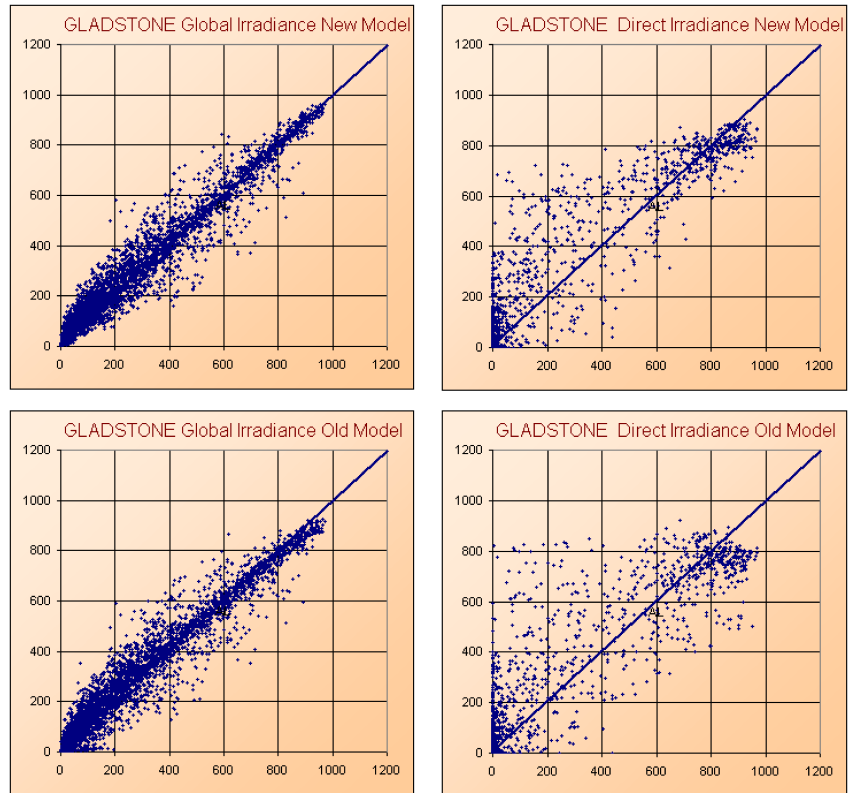


Figure 7: Comparing hourly estimates from satellite (Y axis bottom left) and from a neighboring measurement station (Y-axis top right) to ground measurements. The plot at bottom right shows neighboring station estimation error increase as a function of distance. The red horizontal line represents satellite estimation error.

## **II. 4 Data Preparation**

We processed and produced five years of hourly global and direct irradiance data for the entire Pacific Northwest region. The extent of this region may be seen in Fig. 8.

Hourly records were produced for every location representing a total of ~ 10,500 points for five years.

Results delineate strong microclimatic differences throughout the region. These features had been partially identified through existing measurement programs, but not yet fully delineated.

This new information is being and will be used by Frank Vignola and his team at the University of Oregon to prepare end use products, to conduct site-time specific investigations, and to enhance solar resource knowledge in the professional community with the goal of promoting rational and optimal deployment of solar technologies.

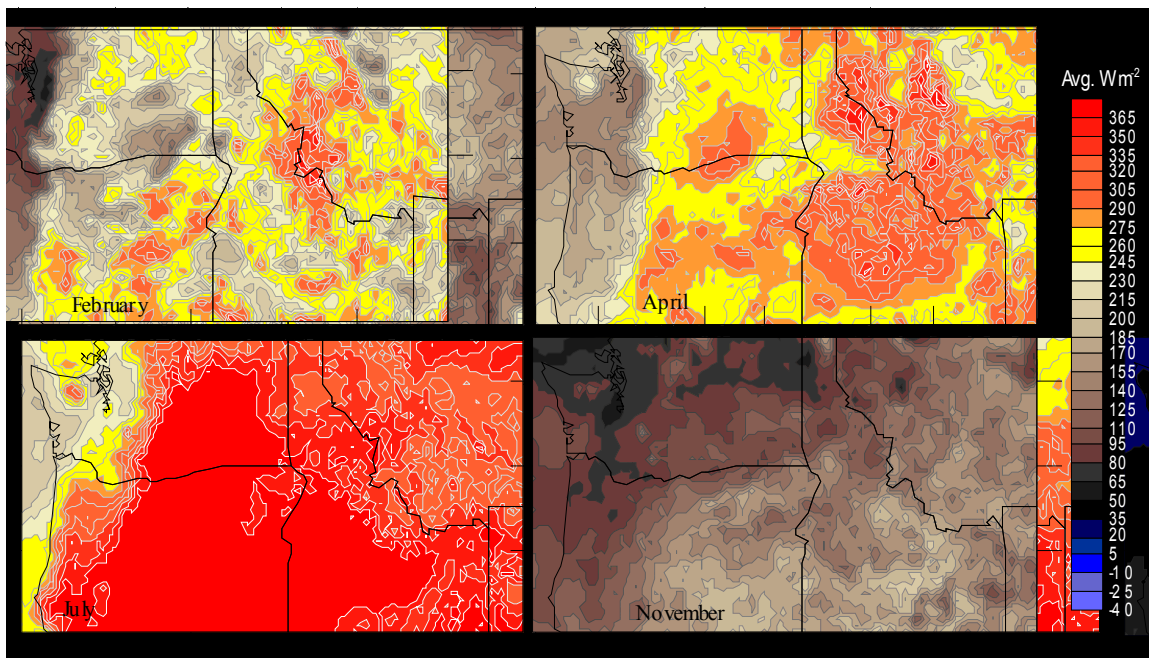


*Figure 8 Example of satellite-derived solar resource maps [average direct irradiance for the months of February, April, July and November 2000]*

### III. Further Validation of the Satellite Derived Data

It is important to understand the data quality that is used in evaluating, modifying and validating a model. The ground base data in this project came from several high quality stations in the UO SRLM solar monitoring network. These stations are equipped with an Eppley Precision Spectral Pyranometer (PSP) and an Eppley Normal Incident Pyrheliometer (PSP) and monitored with Campbell Scientific CR-10 data loggers. The Eppley PSPs at Burns, Hermiston, and Eugene monitoring stations were mounted on ventilators that helped keep dust, snow, and ice from the instruments. In Eugene, the diffuse irradiance was also measured using Schenk Star pyranometer mounted on an automatic tracker with a shade ball.

Because of systematic errors in the cosine response of pyranometers, the global irradiance can be more accurately obtained by projecting the direct normal beam irradiance onto the horizontal surface and adding the diffuse irradiance (Eqn. 1). Using a “star” or “black and white” pyranometer further improves the accuracy of the diffuse measurement by mostly eliminating the re-radiation of PSP pyranometers into the sky on clear days.

$$\text{Global} = \text{Beam} * \text{Cos}(\theta) + \text{Diffuse} \quad \text{Eqn. 1}$$

Where  $\theta$  is the zenith angle.

Before evaluating the satellite derived data it is important to look at some of the limitations of the dataset. The precision of the satellite derived data values was 6 Watts hours per meter squared or 6 W/m<sup>2</sup>. Therefore, irradiance when the zenith angle was above 87.25 degrees was set to zero. For Kimberly, Idaho in 2002 there were 4166 hours when the sun was above 2.75° above the horizon (with refraction this would be about 3°). It would be really difficult to interpret images when the sun is near the horizon. However, this does caused a small systematic error by assuming that the radiation values are zero. Of the 368 hours with the low solar angles, about 1/3<sup>rd</sup> have measured solar irradiance of zero, but the other 2/3<sup>rd</sup>s have measurable irradiance that average 23 W/m<sup>2</sup> during this period. Overall this is very small as this systematic error would lead to a bias error of about -1.3 W/m<sup>2</sup>, especially considering the precision of 6 W/m<sup>2</sup>.

In order to evaluate any model it is important to have a data set not used in the modeling process for an independent test of the model. In January of 2002, a high quality solar radiation monitoring station was installed at Kimberly, Idaho. These data were not used in validating or improving the satellite model and they are used here to evaluate the satellite model and point out the strengths and some weaknesses in the satellite data sets.

There are 329 hours without satellite data that had to be interpolated. This was done by calculating the clearness index for the next valid hour and assuming that the clearness index was constant. The clearness index is the global irradiance divided by the equivalent irradiance outside the earth’s atmosphere. These hours will be included in the analysis, but lead to a slightly larger uncertainty.

The simplest comparison is a plot of the hourly irradiance values as shown in Figs. 9-11 for global, beam, and diffuse irradiance. The irradiance calculated from the satellite data match the ground based measurements fairly well until about the 20<sup>th</sup> of the month. From that point on,

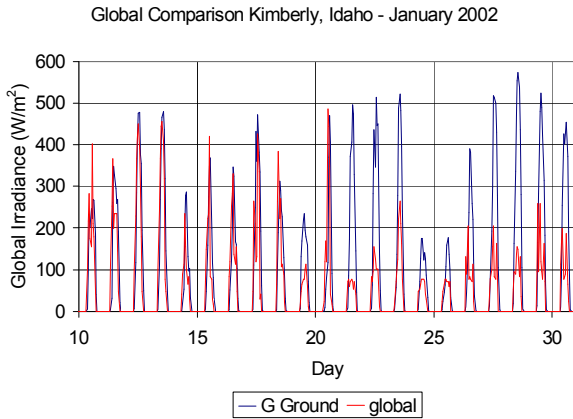


Fig. 9: Comparison of global irradiance as determined from satellite measurements and from ground based measurements.

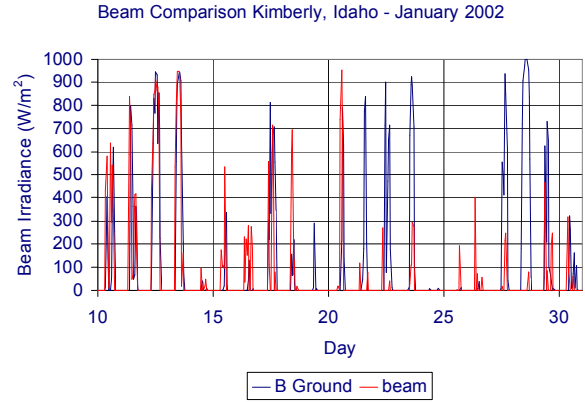


Fig. 10: Comparison of beam irradiance as determined from satellite measurements and from ground based measurements.

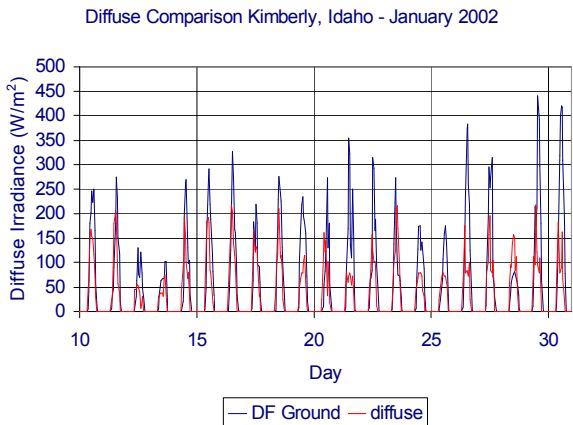


Fig. 11: Comparison of diffuse irradiance as determined from satellite measurements and from ground based measurements.

there seems to be a fairly large discrepancy. This is particularly true on the 29, where Fig. 10 shows a clear day and the satellite measurement shows a complete cloudy day. The cause of this problem is very likely snow frost on the ground. The maximum ground temperature on the 29<sup>th</sup> was  $-5.3^{\circ}\text{C}$  and at night it got down to  $-15^{\circ}\text{C}$ .

The problem cause by snow cover can be seen when comparing the difference between the satellite derived beam irradiance and the ground based measurements as shown in Fig. 12. Note the points in the line that go from 0, 0 to 1000, -1000. These points represent

satellite modeled estimates that are zero when the ground based positive. The winter months of January, February, and December are represented by blue circles and the rest of the year by red Xs. Note that most of the points along the zero satellite value line are from the winter months.

The black trend line in Fig. 12 shows that the average difference between ground based measurements and satellite derived values is less than  $100\text{ W/m}^2$  and is fairly independent of beam irradiance. The problem with snow tends to pull the median down for clear day beam values (those values around  $1000\text{ W/m}^2$ ).

Figs. 13-14 are similar to Fig. 12, except they are for global and diffuse irradiance. There is an excellent match between the average global values from satellite and ground based measurements (See the trend line in Fig. 13). The diffuse values from the satellite model values is obtained by subtracting the beam irradiance projected onto a horizontal surface from the global irradiance shows a marked trend for high diffuse values with the satellite modeled data underestimating the diffuse irradiance. Diffuse values are very sensitive to beam and global

Delta Beam versus Beam Irradiance  
Kimberly, Idaho 2002

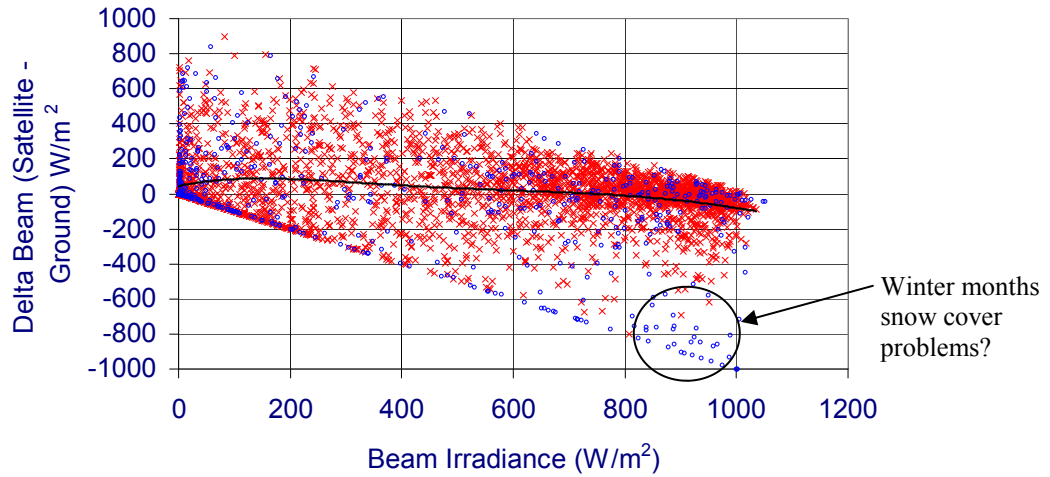


Fig. 12: Difference between beam irradiance obtained from satellite modeling and ground based measurements. Small blue circles are January, February, and December data points. The red X's are data from the rest of the year. The black line is the trend line.

values, so improving the diffuse results might be a way of improving the global and beam irradiance results.

Overall the mean bias errors and standard deviations are given in Table 1. These values are typical of values found in Perez [1]. The term Mean Bias Error (MBE) is a little misleading because the ground based measurements are looking at one point in the sky and the satellite pixels used to estimate the solar irradiance spans a much larger area (about 100 sq kilometers). So the deviation between the two could be fairly large on partially sunny days. The deviation should be much small on cloudy and on sunny days. This can be seen in Figs. 12-14.

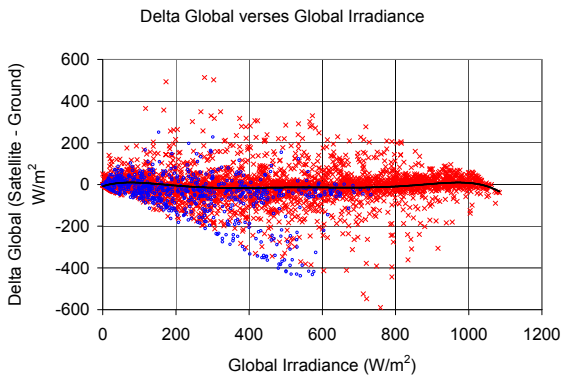


Fig. 13: Difference between global irradiance obtained from satellite modeling and ground based measurements. Blue circles January, February, and December. Red Xs rest of year.

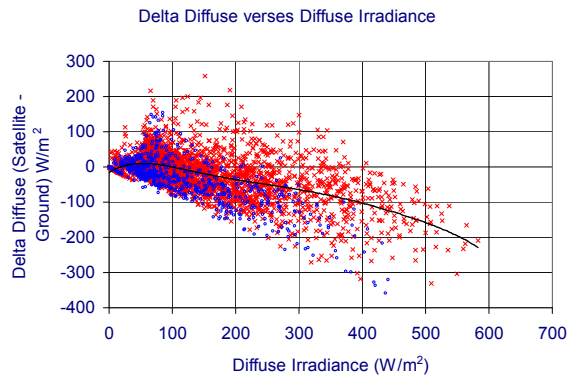


Fig. 14: Difference between diffuse irradiance obtained from satellite modeling and ground based measurements. Blue circles January, February, and December. Red Xs rest of year.

Table 1: Overall bias and deviation between satellite derived values and ground based measurements for Kimberly, Idaho 2002

Irradiance\measure	MBE W/m <sup>2</sup>	MBE %	$\sigma$ W/m <sup>2</sup>	$\sigma$ %
Global	413	-4.9	84	21.5
Beam	481	2.0	200	40.9
Diffuse	132	15.4	60	54.2

values and the ground based measurements for the global, beam, and diffuse irradiance. The

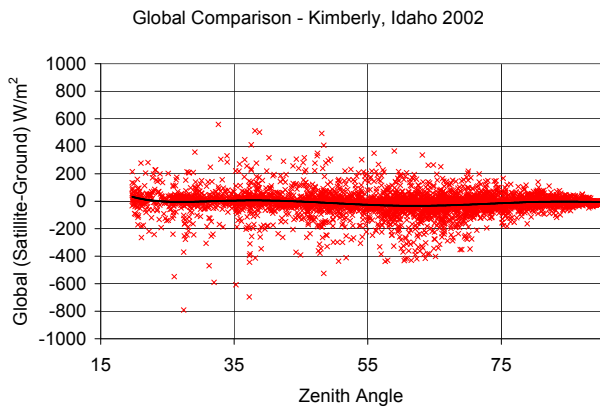


Fig. 15: Comparison of satellite derived global irradiance to ground based measurements against zenith angle.

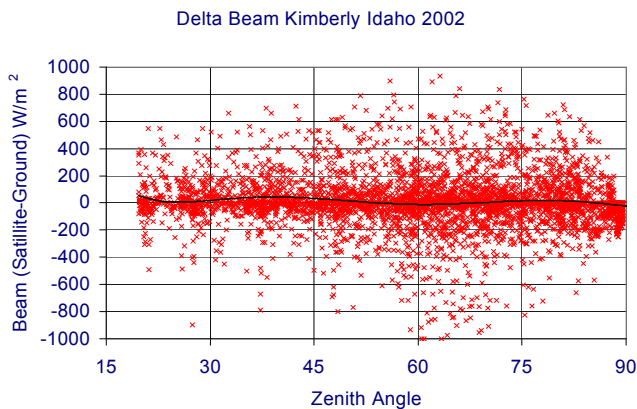


Fig. 16: Comparison of satellite derived beam irradiance to ground based measurements against zenith angle.

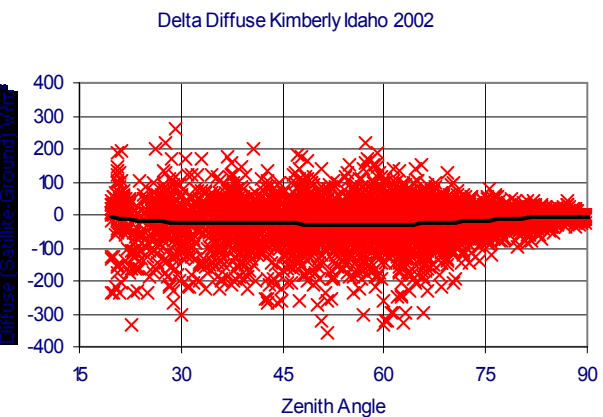


Fig. 17: Comparison of satellite derived diffuse irradiance to ground based measurements against zenith angle.

Another way to look at the difference between the satellite derived and ground based data is to plot the difference against zenith angle (the angle between the perpendicular to the sky and the position of the sun). At sunset the zenith angle is 90° or looking at it another way, 90° - zenith angle is the solar elevation. Figs. 15-17 show the difference between the satellite derived

values and the ground based measurements for the global, beam, and diffuse irradiance. The black line in each plot is a trend line. Note that there the modeling technique has taken account of the zenith angle dependence. Kimberly is not a location used to develop the method to adjust for sun angle differences and this is a good test that this part of the modeling works well.

Again, the diffuse values determined from the global and beam irradiances from the satellite model underestimate the diffuse value. The diffuse values from Kimberly are about 20 W/m<sup>2</sup> higher than those from Burns or Hermiston on average because the diffuse values are obtained by measurements with a “star” type pyranometer with a shade disk. At Burns and Hermiston, the diffuse values are calculated from the beam and



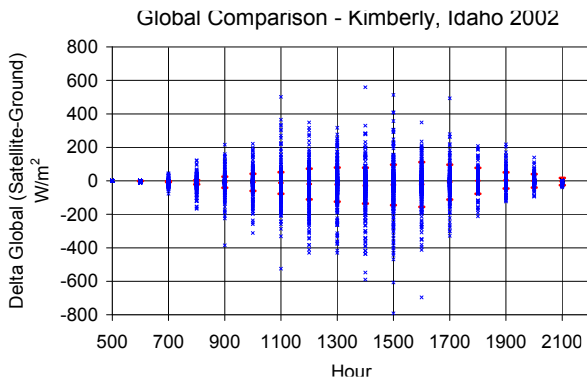


Fig. 18: Plot of difference between satellite derived and ground based measurements of global irradiance plotted against time of day. Red bars represent standard deviation.

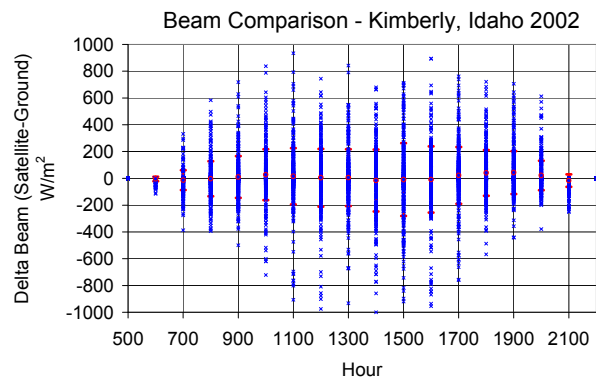


Fig. 19: Plot of difference between satellite derived and ground based measurements of beam irradiance plotted against time of day. Red bars represent standard deviation.

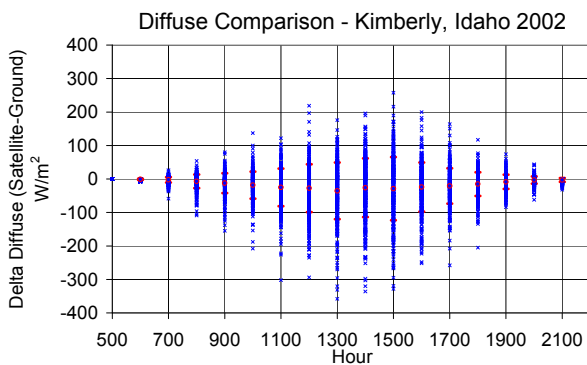


Fig. 20: Plot of difference between satellite derived and ground based measurements of diffuse irradiance plotted against time of day. Red bars represent standard deviation.

global data and have systematic errors. The fact that the satellite derived diffuse values are low by about  $20 \text{ W/m}^2$  on average may be attributed to the global values being low by about the same amount. Right now this is speculation and future work is needed to see if this trend also exists at other locations around the world.

Another test is to examine the deviation across the day. These plots are shown in Figs. 18-20. The small deviations during the first hour in the morning and the last hour in the evening is a little misleading. During most of the year, there is no incident radiation during these morning or evening hours. The amount of radiation is small, but future models

should look into ways to estimate incident solar radiation during these time periods when there are extremely low solar angles.

Overall, the satellite derived solar radiation provides a good estimate of the solar resource over large areas. The data values have similar statistics and means as ground based measurements and will prove just as useful for most applications. Having the mean bias errors of less than 5% is remarkable, especially with the absolute accuracy of ground based measurements of 3% for the very best of maintained solar monitoring stations. Much of the standard deviation between the measurements is expected because of the differences in measurements. Some improvements are probably possible by tweaking the process but the gains are small and will be gained only with considerable effort. For example, better techniques are needed to distinguish icy or snowy conditions from ground fog and clouds.

Improvements in estimation of beam irradiance will depend on other better measurements of

turbidity. Again these gains will be small because the mean bias errors and standard deviations are small.

There is a system underestimation of the diffuse irradiance calculated from the satellite derived global and beam irradiance values. Work in the future is needed to clarify the cause of this discrepancy. The numbers are a very small part of the value of global or beam irradiance, but are significant for diffuse measurements. One possibility is that the models used to estimate the global irradiance used ground based data obtained from pyranometer measurements that had a systematic error. That error is the re-radiation into the sky by the pyranometers.

#### IV. Production of Solar Resource Maps

Monthly average irradiance maps were created for the Pacific Northwest by averaging the monthly irradiance from 1998-2002. The average was used instead of selecting the typical year because the average beam irradiance has been increasing over the last 25 years and 2002 had the highest beam irradiance on record (See Fig. 21). The monthly average values were feed into an Arc-Info program to generate detailed maps of the region. An elevation algorithm was used to smooth the 10,500 plus data points to generate the final maps. Global, beam, and diffuse maps were created for all 12 months and for the yearly average. Copies of the maps are given on the DVD along with the data used to derive the maps. In addition, the printouts of the maps are included with this report.

One difficulty with developing the maps was to determine a scale that would work for the wide variety of irradiance value encountered and at the same time show the variations around the

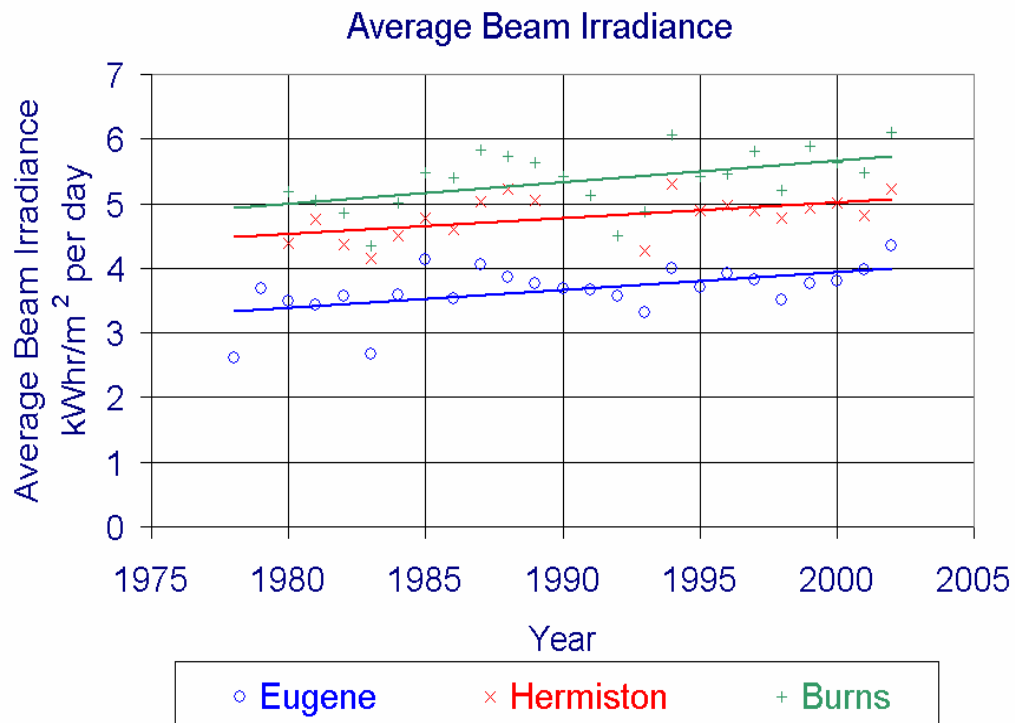
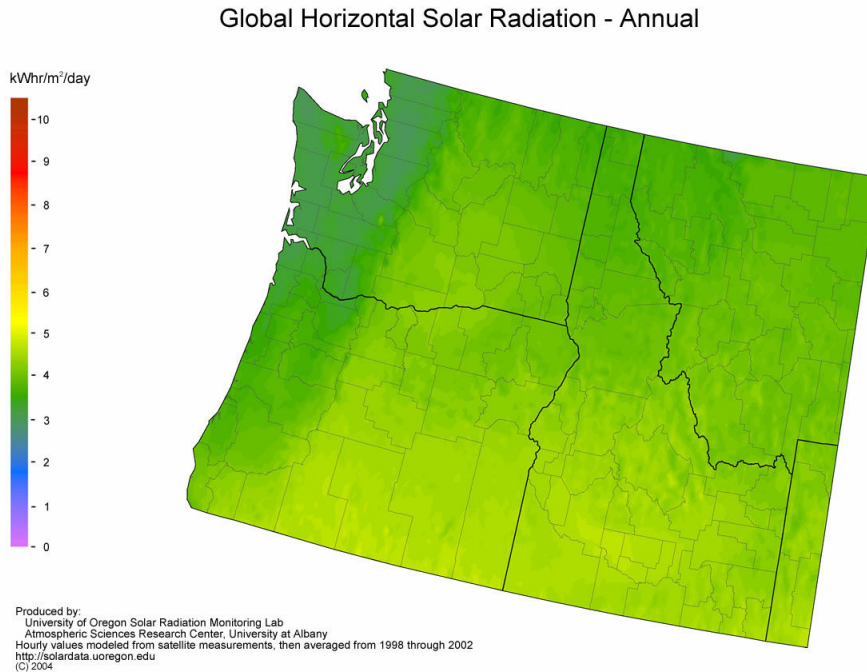


Fig. 21: Change in yearly average beam irradiance from 1978 through 2002 for the three stations that have long term beam measurements in the UO SRML Solar Monitoring Network.



*Fig. 22: Solar resource map of the annual global irradiance. A map of the annual beam irradiance is shown on the cover of this report.*

region. In addition, only one scale was desired to work for all maps (Fig. 22).

Such features as the effects of the Cascade mountain range show up clearly on these maps as well as rain shadows caused by mountains. The sunniest areas in the region are only receive about 40% more global irradiance than the cloudiest.

## V. Structure of the Database

As produced, the database came as one set of values for the whole region for each hour over 5 years. This is the natural for from transforming the satellite pictures into irradiance values. This flat structure was transformed into a continuous data stream for each year for each pixel represented in the database. Each data set is identified by the latitude and longitude of the middle of the group of pixels used to produce the data. The longitudes and latitudes were separated by  $0.1^\circ$  and the file were given the a name represented by the coordinates. The last two digits of the year were also included in the name of the file. For example, 01113\_15\_45\_25.txt is the name of the data set presenting 2001 at  $-113.15$  longitude and  $45.25$  latitude. The first 24 hours of the data set are shown in Table 2.

The data files are tab separated ASCII files for easy import into spread sheets. The first line in the data file contains header information and the following lines contain data for each hour of the year. The site number is identified with the longitude and latitude (113154525 in this example). The helps with identification of the file in case the name is changed or corrupted. The second piece of data is the year (2001 in this example), followed by 'global', 'beam', 'diffuse', 'flag', and 'cflag'. These words identify the data type in the column below.

The data column starts with the day of the year, followed by the time (based on UTC or Greenwich mean time), the global, beam, and diffuse data values, followed by two flag numbers. The first flag indicates whether the data came directly from satellite photos or had to be interpolated from following values. If the flag was 1, either the sun was below the horizon

Table 2: First day of the 2001 yearly dataset for location -113.15 Longitude and 45.25 N Latitude

113154525	2001	global	beam	diffus	flag	cflag
1	100	0	0	0	0	0
1	200	0	0	0	0	0
1	300	0	0	0	0	0
1	400	0	0	0	1	0
1	500	0	0	0	1	0
1	600	0	0	0	1	0
1	700	0	0	0	1	0
1	800	0	0	0	1	0
1	900	0	0	0	1	0
1	1000	0	0	0	1	0
1	1100	0	0	0	1	0
1	1200	0	0	0	1	0
1	1300	0	0	0	1	0
1	1400	0	0	0	0	0
1	1500	0	0	0	0	0
1	1600	78	258	51	0	0
1	1700	42	0	42	0	0
1	1800	282	564	104	0	0
1	1900	192	108	153	0	0
1	2000	192	90	159	0	0
1	2100	228	306	127	0	0
1	2200	222	678	53	0	0
1	2300	96	468	33	0	0
1	2400	0	0	0	0	0

and no picture was available or that the picture was not retrievable. If the flag was one during the time when solar irradiance was incident on the area, then the clearness index of the next possible value was used to fill in the missing data. This enable a complete hourly data set to be constructed for the whole time period.

The final flag value indicated the quality of the data point. The higher the value, the more uncertain the data value.

## VI. Solar Angle and PV Performance Calculator

A solar angle calculator and photovoltaic performance calculator were developed to facilitate the used of the database. The calculator is an Excel add-in that written in Visual Basic and provides for easy analysis and calculation. To use the calculator, a data file has to be imported into Excel and the calculator set for the given location. The data files were written in tab separated ASCII to be directly importable into Excel.

The calculator was demonstrated at the Solar Summit in October 2003 to state energy office personnel, utility personnel, solar contractors, to others interested in solar energy. An html file explains the use of the calculator and is given in Appendix B of this report. The html file and the calculator are included on a CD given with this report.

The calculator is based on two software packages available from NREL. The first is the

solar position calculator called "sunpos". This was translated from the c code to visual basic. Next, the code for PVWatts was added to this calculator to estimate the performance of photovoltaic systems at all tilts and orientations along with one axis and two axis tracking. In the process one error was found in the PVWatts program and this information was forwarded to NREL and the author of the software program. While the change was minimal and only affected systems that were nearly horizontal, the changes were incorporated into the PVWatts program.

With the database and the solar calculator, an estimate of solar electric system can be calculated for any location in the Northwest. The UO SRML is currently under contract with the Energy Trust of Oregon to monitor the performance of six photovoltaic systems in Oregon.

Information from this monitoring project will be evaluated, and if appropriate, incorporated into the solar calculator to improve the estimates.

In addition, the software also calculates a wide of other solar parameters from clearness index to the cosine of incident angles. These values, can be used as input to various solar related models. On such application, is the correlation of solar irradiance into solar illuminance. In the future it should be possible to incorporate some of these other models directly into the solar calculator.

A program called Install.xls has been created that automatically installs the solar calculator as an add-in to Excel on a windows based computer. To install the solar calculator, put the CD into the disk drive and double click on Install.xls. Then follow the instructions. This program has been tested on several version of Excel and Window operating systems, but users can give us a call if the installation program doesn't work. The future plan is to make this program available as shareware on the UO SRML web site.

## **VII. Distribution of the Database**

The state energy offices of Oregon, Washington, and Idaho were sent a DVD with all the satellite derived solar radiation data for their state along with daily and monthly average data files. In addition the regional monthly average and annual maps were included on the DVDs. Three DVDs are included with this report contain all the data given to the state energy offices and the data from western Montana and northwestern Wyoming that were also analyzed. In addition, the ground based data collected by the UO SRML solar monitoring network through 2002 was included on the DVDs.

Also included in the distribution are papers showing how to calculate illuminance from irradiance data. As in the past, we will be working with the regional energy offices to help them make full use of this data.

## **VIII. Conclusions**

Solar resource assessment has taken a giant step forward in the Pacific Northwest. It is now known how the resource varies across the region on a very fine scale. The data have been sent to the energy offices of Idaho, Oregon, and Washington so that they can include the data in their GIS systems. The data will shortly be given to the National Renewable Energy Laboratory, the Bonneville Power Administration, the Northwest Power and Conservation Council, the Eugene Water and Electric Board, and the Energy Trust of Oregon. Maps derived from the new database are available over the Internet and for individual locations will be made available upon request.

This high density data, when combined with high quality data being collected by the UO SRML solar monitoring network forms a solid basis for planning the development and integration of the solar resource in the region. While a longer-term database is needed to analyze the climatic trends and variations of the solar resource, over twenty five years of data have been collected at high quality data sites. Using these sites as reference sites, the climate trends observed at these sites can be translated into the surrounding areas with a fair degree of confidence by using the database that has been developed under this project.

NREL is evaluating the upgrade of the National Solar Radiation Data Base. Data produced on

this project will be shared with NREL in their efforts to determine the best way to upgrade the NSRDB and to test the models and methods used in this effort.

More importantly, several improvements have been made to the satellite model itself. Several steps have been added to the modeling procedure that have refined the model. In addition, this project has helped develop techniques to estimate the beam irradiance from satellite data as well as global irradiance. This is an important step, because accurate modeling of the beam irradiance is critical to accurate modeling of the incident solar radiation and for concentrating systems.

As we move further into the information age, developing methods to determine incident irradiance over vast areas with fine details will enhance the planning and managing of resources. This project will show what can be done and give the state energy offices to the database from which future tools can be developed.

# Appendix A – Satellite to Irradiance Models

## Appendix A. 1 -A New Operational Satellite-to-Irradiance Model Description, Validation

Richard Perez<sup>1</sup>  
Pierre Ineichen<sup>2</sup>  
Kathy Moore<sup>1</sup>  
Marek Kmiecik<sup>1</sup>  
Ray George<sup>3</sup>  
Frank Vignola<sup>4</sup>  
{{Qi Long Min<sup>1</sup>??}}

### 1. Introduction

Geostationary satellites monitor the state of the atmosphere and the earth's cloud cover on a space-and-time continuous basis with a ground resolution approaching 1 km in the visible range. This information can be used to generate time/site specific irradiance data and high-resolution maps of solar radiation

Compared to ground measurements, satellite-derived hourly irradiances have been shown to be the most accurate option beyond 25 km from a ground station (Zelenka et al., 1999). Another noted strength of the satellite resides in its ability to accurately delineate relative differences between neighboring locations, even though absolute accuracy for any given point may not be perfect; hence satellites have proven to be a reliable source of solar microclimate characterization.

Simple satellite models derive a cloud index (CI) from the satellite visible channel and use this index to modulate a clear sky global irradiance model that may be adjusted for ground elevation and atmospheric turbidity. In this paper we present an evolution of such a simple satellite model (Zelenka et al., 1999) with the objective of addressing observed remaining weaknesses.

### 2 Old Model

#### 2.1 Global irradiance (GHI)

This model is an evolution of the original Canot et al. model (1986), based upon the observation that shortwave (i.e. solar) atmospheric transmissivity is linearly related to the earth's planetary albedo (Schmetz, 1989) sensed by the satellite as earth's radiance and reported as an image-pixel count.

The model includes two distinct parts:

- (1) pixel-to-cloud index (CI) conversion;
- (2) CI to global irradiance conversion.

<sup>1</sup> ASRC, The University at Albany, Albany, New York

<sup>2</sup> CUEPE, University of Geneva, Geneva, Switzerland

<sup>3</sup> NREL, Golden, Colorado

<sup>4</sup> University of Oregon, Eugene, Oregon

Pixel-to-cloud index conversion: Image pixels are received as “raw” pixels which are proportional to the earth’s radiance sensed by the satellite. A raw pixel is first normalized by the cosine of the solar zenith angle to account for first order solar geometry effect. This normalized pixel is then gauged against the satellite’s pixel dynamic range at that location to extract a cloud index (Fig. 1). The dynamic range represents the range of value a normalized pixel can assume at a given location from its lowest (darkest pixel, i.e., clearest conditions) to its highest value (brightest pixel, i.e., cloudiest conditions). The dynamic range at a given location is maintained by the flux of incoming normalized pixels at that location. While the upper bound of the range remains constant (except for a time-line modulation to account for satellite’s calibration drift), the lower bound evolves over time as a function of the local ground albedo variations (chiefly snow, moisture, and vegetation effects). Incoming pixels within a sliding time window are used to determine this lowest bound. The old model uses an 18-day window in summer and a shorter 5-day window in winter in an attempt to capture fast evolving snow cover variations. The lower bound is determined as the average of the 10 lowest pixels in the sliding time window. Before being considered for dynamic range maintenance, an incoming pixel is subjected to a secondary normalization to account for a secondary atmospheric air mass effect and for the hot spot effect (Zelenka et al., 1999). The latter is a function of the sun-satellite angle and incorporates both atmospheric back-scatter brightness intensification and the fact that ground surface becomes brighter as the sun-satellite angle diminishes due to the reduction of ground shadows seen by the satellite (e.g., Pinty and Verstraete, 1991). This secondary normalization is then applied in reverse to the lower bound of the dynamic range before it can be compared to an incoming normalized pixel for the determination of the cloud index as

$$CI = (norpix - low^*) / (up - low^*)$$

where norpix is the cosine-normalized image pixel, up is the dynamic range’s upper bound and low\* is the lower bound after reverse secondary normalization.

Cloud-index-to-GHI Conversion: GHI is determined by:

$$GHI = (0.02 + (1 - CI)) Ghc$$

Where Ghc is the clear sky global irradiance per Kasten (Kasten, 1984). Gc is adjustable for broadband turbidity as quantified by the Linke turbidity coefficient (Kasten, 1980), and ground elevation.

$$Ghc = 0.84 I_0 \cos Z \exp \{ -0.027 am [ \exp(-alt/8000) + (TL-1) \exp(-alt/1250) ] \}$$

Where I<sub>0</sub> is the extraterrestrial normal incident irradiance, Z is the solar zenith angle, am is the elevation-corrected air mass, TL is the Linke turbidity coefficient and alt is the ground elevation in meters.

## 2.2 Direct irradiance (DNI)

DNI is modeled from the satellite-derived global using the model DIRINT originally developed and validated for ASHRAE (Perez et al., 1992). This model is an evolution of NREL’s DISC model, using a “stability index” derived from the consecutive records of GHI input.

## 2.3 Observed shortcomings of the old model



- Model bias: Although overall bias for GHI has generally been found to be acceptable, there remains important seasonal and regional disparities.
- Snow cover: The short winter-time sliding window to detect rapid albedo changes caused by snow cover in northern locations leads to diminished model performance, sometime resulting in large winter biases.
- DNI: DNI is extracted from global using a secondary model that had not been developed to fully account for regional turbidity and ground elevation.
- Climate: although the model works relatively well overall in “generic” temperate climates, limitations have been observed in more extreme climates, particularly in very clear arid locations found in the southwestern US, where the models tend to underestimate irradiances (in particular DNI).

### 3. New Model

#### 3.1 Pixel to cloud index

The new model features two major evolutions: (1) the utilization of external information for snow cover and (2) an accounting of sun-satellite angle effects individualized for each pixel. A seasonal trend adjustment of the dynamic range’s lower bound and a minor modification of the secondary airmass effect normalization are also introduced.

Snow cover: For the USA and parts of Canada, the NOHRSC (2002) maintains a daily report of ground snow cover that is accessible via the Internet. The data are made available on a grid of resolution comparable to our satellite archive. The data may be of three types: (a) no snow cover, (b) snow cover and (c) too cloudy to tell. The satellite model uses this information by resetting the value of the dynamic range’s lower bound if a pixel’s location switches from no-snow cover to snow cover. This implies dropping the current lower bound and replacing it by the value of new incoming lowest pixels. As these pixels get lower as snow ages and melts, the lower bound naturally regains its snow-free value. This process is illustrated in Fig. 2.

Dynamic range lower bound: Using the external snow cover information frees the model to use a longer time window for the dynamic range in winter. The current model uses a year-around 60-day window which allows a robust determination of the lower bound with many data points. The actual minimum is the average of the ten lowest normalized pixels over this time window. The switch to a longer year-around window was facilitated by introducing a small trend correction,  $\zeta$ , based upon the observed mean seasonal variation of the lower bound (e.g., see the seasonal trend in Fig. 3)

$$\zeta = (3 + 0.5 \cos(\text{doy} \pi/365)) / (3.0 + 0.5 * \cos((\text{doy} - \text{win} / 2) \pi/365))$$

with:           doy = day of year, and win = time window length in days

Sun-satellite angle effects: In the old model we had attempted to account for this effect by using a generic normalization function applicable to all pixels. It soon became apparent that there were strong differences from pixel to pixel, associated with ground cover and soil nature. The largest cause of these differences had been overlooked: specular reflectivity of the ground surface. This effect is particularly significant in dry western regions of North America and can vary substantially over short distances. Fig. 3 compares the minimum dynamic ranges traces for Albuquerque, New Mexico, for a morning and a mid-afternoon hour. Using a single lower-

bound trace for all points, as in the old model, led to strong mid-afternoon underestimations because naturally brighter afternoon pixels were misinterpreted as having a higher cloud index. This shortcoming was resolved by deriving a unique, different function for each pixel relating each hour's relative minimum to the day's lower bound. Operationally, these individual pixel functions consist of month-by-hours lookup tables derived from several years of archived satellite data.

### 3.2 GHI generation

As in the old model cloud indices are used to modulate a clear sky global irradiance model that may be adjusted for both broadband turbidity and ground elevation. However, several modifications have been introduced.

Broadband turbidity: Ineichen and Perez (2002) recently proposed a revised formulation of the Linke Turbidity coefficient to remove its dependence on solar geometry. This new formulation was used to generate a seasonal grid of TL for the North American continent, based upon gridded climatological aerosol, ozone and water vapor data that had previously been assembled for the preparation of the NSRDB (1995). The new formulation could also be used, as appropriate, to generate TL "on the fly" from regional ground monitoring stations (e.g., from DNI measurements).

Clear-sky global irradiance: The Kasten clear sky model was modified to exploit the new turbidity formulation and to improve its fit of very clear / high elevation locations found in the western part of the continent, while conserving its representativeness of standard temperate environments.

$$Ghcnew = cg1 \text{ lo } \cos z \exp(-cg2 \text{ am } (fh1 + fh2 (TI - 1))) \exp(0.01 * am^{1.8})$$

With

$$\begin{aligned} cg1 &= (0.0000509 \text{ alt} + 0.868) \\ cg2 &= 0.0000392 \text{ alt} + 0.0387 \\ fh1 &= \exp(-\text{alt} / 8000) \\ fh2 &= \exp(-\text{alt} / 1250) \end{aligned}$$

Cloud-index function: The linear CI-to-GHI function was dropped in favor of a form representative of observed data. The present formulation, plotted in Fig. 4, is a fit to five environmentally distinct, very high quality ground truth stations (Albany, NY, Burlington, KS, Eugene, Gladstone and Hermiston, OR).

$$GHI = Ktm \text{ Ghcnew } (0.0001 Ktm \text{ Ghcnew } + 0.9)$$

With

$$Ktm = 2.36 \text{ CI}^5 - 6.2 \text{ CI}^4 + 6.22 \text{ CI}^3 - 2.63 \text{ CI}^2 - 0.58 \text{ CI} + 1$$

### 3.3 DNI generation

DNI is obtained, as GHI, via modulation of clear-sky direct irradiance. The clear sky irradiance model was recently introduced by the authors as part of the development of the new TL formulation (Ineichen and Perez, 2002):

$$Bc = \text{Min} \{ 0.83 \text{ lo } \exp(-0.09 \text{ am } [TL - 1]) (0.8 + 0.196 / \exp[-\text{alt} / 8000]), \\ (Gcnew - Dc) / \cos Z \}$$

where DC is the minimum clear sky diffuse irradiance given by:

$$D_c = G_{cnew} \{ 0.1 [1 - 2 \exp(-TL)] \} \{ 1 / [0.1 + 0.882 / \exp(-\text{elev} / 8000)] \}$$

Unlike GHI, the direct modulating factor is not derived from CI but from global, using the global-to-DNI model, DIRINT (Perez et al., 1992), in a relative mode -- thereby doing away with the absolute accuracy limitation of the model, but retaining its stability index capability.

DNI is obtained from:

$$B = \lambda B_c, \quad \text{with } \lambda = \text{DIRINT (GHI)} / \text{DIRINT (G}_{h\text{clear}})$$

We had initially planned to derive DNI directly from CI and use a “one step” model similar to that of global (Ineichen and perez, 1999, Ineichen et al., 2000). The decision to rely partly on DIRINT and to model B via global stems from the capability of this model to make use of consecutive GHI records to estimate a stability index and adjust modeled DNI based upon this parameter, with appreciable impact on model accuracy.

### 3.4 Operational model

While the modeling process has been thoroughly described above, the operation of the model on a geographic scale, either for the preparation of maps or site/time specific time series requires some degree of logistics and information processing. This logistical approach is summarized in Fig. 5. It includes several layers of gridded information. The grid size of our current archive is 0.1 degrees latitude-longitude. Ultimate achievable resolution of visible channel GOES image could approach 0.01 degree. The information gridded layers include:

- Raw satellite pixels (visible channel) obtained via direct processing of primary GOES east and GOES west satellite images. We archive gridded raw pixel frames on an hourly basis.
- Terrain elevation
- Climatological Linke turbidity – 12 monthly layers, derived from previously gridded aerosol optical depth data (NSRDB, 1995)
- Snow cover – daily gridded frames from (NOHCRS, 2002)
- Specular correction factor – 216 layers (12 months by 18 hours) derived from the hourly processing of 5 years worth of raw pixel data.

## 4. Validation

### 4.1 Experimental Ground Truth Data

A total of ten stations, listed in Table I are used to evaluate model performance. As mentioned above data from five of these stations (\*) were used to fit the CI-to-global transfer function. Most of the stations follow rigorous calibration and quality control protocols, particularly those directly or indirectly affiliated with the ARM (2002) or BSRN (2002) programs and with the Pacific Northwest network.

Site	Climate	Notes
Albany, NY (1999)	Humid continental	BSRN
Burns, OR (1999-2000)	Semi-arid, high elev.	Pacific Northwest network ....
Albuquerque, NM (1999)*	Arid, high elevation	Sandia Natl. Labs, ARM protocol
ARM-Burlington, KS (1999)	Dry continental	ARM
Eugene, OR (1999)	Temperate	Pacific Northwest network
FSEC-Cocoa, FL (1999)	Subtropical	Florida Solar Energy center
Gladstone, OR, (part-1999)	Temperate, humid	Pacific Northwest network
Hermiston, OR (1999-2000)	Temperate, dry	Pacific Northwest network
Klamath Falls, OR (pt-1999)	Temperate dry	Pacific Northwest network
Kramer Junction, CA (1999)	Arid	SEGS power plant monitoring

Albany, ARM-Burlington and FSEC are used to validate irradiances derived from GOES-East (GOES-8) data. Burns, Eugene, Gladstone, Hermiston, Klamath Falls and Kramer Junction are used for GOES-West (GOES-10). Albuquerque is used to validate irradiances derived from both satellites.

## 4.2 Results

The first set of validation metrics – overall observed root mean square errors (RMSE) and mean bias errors (MBE) – is presented in Table 2. We compare the old model against two versions of the new model: (1) the operational model as described in this paper, and (2) the same with monthly turbidity derived locally from the ground truth DNI measurements. The statistics are based on 96% of the points, rejecting 2% of the most extreme positive and negative differences – most of the highest differences have little to do with model intrinsic accuracy but are mostly reflective of the impact of cloud patterns on the comparison between an instantaneous measurement extended in space - the satellite pixel - and a pinpoint ground measurement extended in time - hourly integration (Zelenka et al., 1999).

The observed performance improvement is systematic for all sites using the RMSE benchmark. This is remarkable since the room for gain is not as large as the magnitude of the initial error would suggest. Because of the above-mentioned pixel-ground station discrepancy and small remaining satellite navigation uncertainties the initial is already close to achievable effective accuracy (Zelenka et al., 1999). As it is, the new model approaches this limit for GHI at several of the sites. Inspection of the MBE benchmark also reveals overall improvement – Note in particular that the strongest underestimations (Albuquerque, Kramer) and overestimations (Gladstone) have been reduced. The model using local measurement-based turbidity shows only slight additional improvement. The case of Florida stands out, with a much stronger initial RMSE and MBE and small accuracy improvement. The causes for this will have to be investigated further. At present the two major suspected causes are (1) the humid subtropical climate with frequent broken cloud patterns, and more likely, (2) the fact Cocoa is situated at the edge of a body of water, with a satellite pixel straddling two very different minimum brightness environments.

Model performance improvement may be qualitatively visualized in Figs. 6 and 7 compare the old and the new (with generic TL) performance in Albuquerque, NM for GOES west. Note that Albuquerque provides a fully independent model test bed as this site was not used to fit the CI-to-GHI index function. The reduction of scatter and high-end bias is particularly striking for DNI. Much of the improvement at that site stems from the utilization of the pixel specific look-up

table describing the local sun-satellite angle effect. In the old model, enhanced brightness of the ground peaking in early afternoon is mistaken as increased cloud index resulting in a severe DNI underestimation. Much of this shortcoming is corrected with the new model.

Overall bias may appear reasonable only to hide seasonal effects that may cancel-out. So, another gauge of model performance improvement is to observe the variations of seasonal biases. Fig. 8 compares the seasonal DNI bias traces for all sites. The new model traces are noticeably more compact showing more site-to-site as well as season-to-season consistency.

## 5. Conclusion

We have presented a new simple model capable of exploiting geostationary satellite visible images for the production of site/time specific global and direct irradiances. The model exhibits systematic performance improvement for all tested locations representing a wide range of climatic environments. As it is, the level of observed RMSE at some of the test stations approaches the effective accuracy limit previously discussed by the authors and colleagues (Zelenka et al., 1999). The new model is particularly efficient at correcting possible distortions resulting from certain types of ground surfaces.

Future work will focus on (1) addressing remaining ground specular effects that may leave a trace in the production of microclimatic solar resource maps; (2) investigating other climates, particularly subtropical and tropical, which have only been marginally covered here; (3) investigating whether additional satellite channels (in particular IR) may lead any noticeable cloud index detection and model performance improvement; (4) comparing this model with other models (e.g., Broesamle et al., 2001) using common ground truth stations as will be done as part of the SWERA program (SWERA, 2002).

*Acknowledgement – This work combines the research and finding of several research programs: NREL Contract NAA-13044102, AXE-0-30070-01, University of Oregon’s Solar Resource GIS Data Base for the Pacific Northwest Using Satellite Data, and UNEP’s SWERA program.*

## REFERENCE

ARM (2002): Atmospheric Radiation Measurement Program, <http://www.arm.gov/>

Broesamle, H., H. Mannstein, C. Schillings and F. Trieb, (2001): Assessment of Solar Electricity Potentials in North Africa Based on Satellite Data and a Geographic Information System. Solar Energy 70, pp. 1-12

BSRN (2002): Baseline Surface Radiation Network, <http://bsrn.ethz.ch/>

Cano, D., J.M. Monget, M. Aubuisson, H. Guillard, N. Regas and L. Wald, (1986): A Method for the Determination of Global Solar Radiation from Meteorological Satellite Data. Solar Energy 37, pp. 31-39

Ineichen, P. and R. Perez, (1999): Derivation of Cloud Index from Geostationary Satellites and Application to the Production of Solar Irradiance and Daylight Illuminance Data Theoretical

and Applied Climatology Vol 64, 119-130.

Ineichen, P., R. Perez, M. Kmiecik and D. Renne, (2000), Modeling Direct Irradiance from GOES Visible Channel Using Generalized Cloud Indices. Proc. 80th AMS Annual Meeting, Long Beach, CA

Ineichen, P. and R. Perez, (2002): A new airmass independent formulation for the Linke turbidity coefficient. Submitted to Solar Energy

Kasten F. (1980): A simple parameterization of two pyrheliometric formulae for determining the Linke turbidity factor. Meteorol. Rdsch. 33, 124-127

Kasten, F., (1984): Parametrisierung der Globalstrahlung durch Bedeckungsgrad und Trübungsfaktor. Annalen der Meteorologie Neue Folge, 20, pp. 49-50

NOHRSC, (2002): National Operational Hydrologic Remote Sensing Center. <http://www.nohrsc.nws.gov/>

NSRDB, (1995): National Solar Radiation Data Base - Final Technical Report, Volume 2, 1995. NREL/TP-463-5784

Perez, R., P. Ineichen, E. Maxwell, R. Seals and A. Zelenka, (1992): Dynamic Global-to-Direct Irradiance Conversion Models. ASHRAE Transactions-Research Series, pp. 354-369

Pinty, B. and M. M. Verstraete, (1991): Extracting Information on Surface Properties from Bidirectional Reflectance Measurements. J Geophys. Res. 96, 2865-2874

Schmetz, J. (1989): Towards a Surface Radiation Climatology: Retrieval of Downward Irradiances from Satellites. Atmos Res., 23, pp. 287-321

SWERA (2002): Solar and Wind Resource Assessment, <http://www.uneptie.org/energy/act/re/fs/swera.pdf>

Zelenka, A., Perez R, Seals R. and Renné D., (1999): Effective Accuracy of Satellite-derived irradiance, Theoretical and Applied Climatology, 62, 199-207

## Figure Captions

Figure 1: Satellite Dynamic Range – GOES-8 southeastern US, 1997-2000. Note the lower bound seasonal variation and the upper bound decrease from satellite calibration decay.

Figure 2: Impact of snow on dynamic range lower bound, Burns, OR, January-May 1999.

Figure 3: Impact of ground specular reflectivity on lower bound. Note that the PM trace is well above of the lower bound calculated accounting only for generic sun-satellite angle effects (original trace).

Figure 4: Illustration of the new CI-to-GHI function

Figure 5: Operational Model data sets.

Figure 6: Modeled vs. measured global irradiance for the old and new model in Albuquerque, NM using GOES-West as model input.

Figure 7: Comparing, measured and modeled typical clear-sky DNI daily profiles in Albuquerque, NM.

Figure 8: Comparing old and new model monthly MBE profiles for all sites.

## Table Titles

Table 1: Ground Truth Stations

Table 2: Model RMSE and MBE for global and Direct Irradiance.

Figure 1

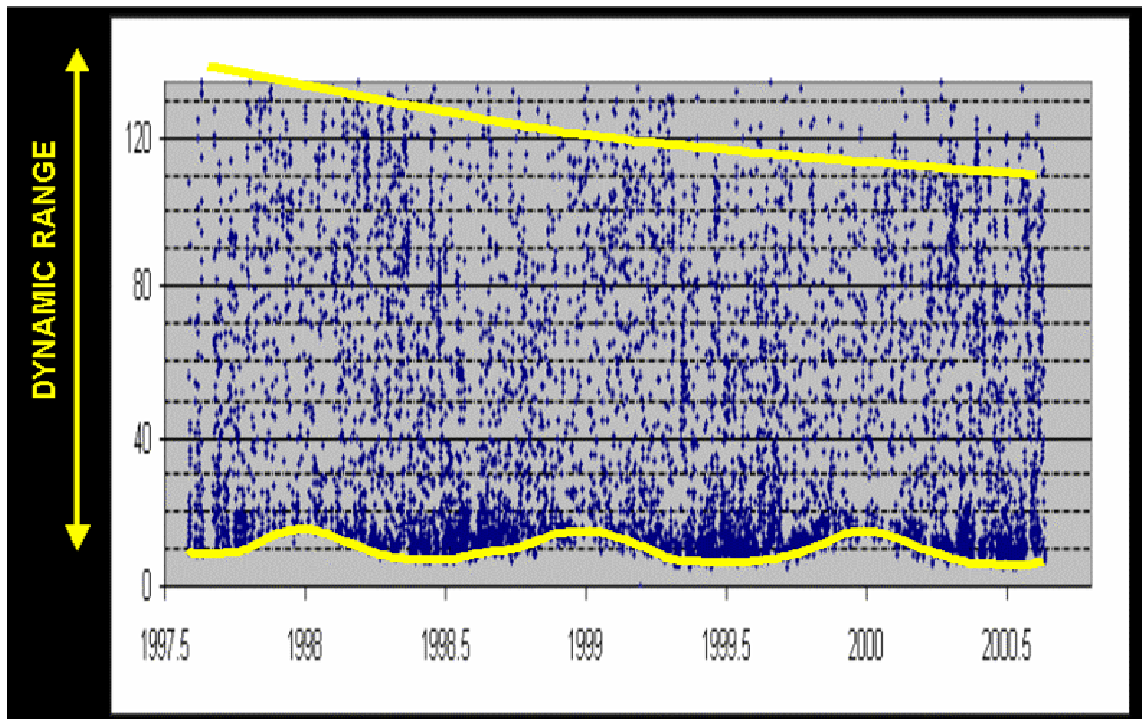




Figure 2

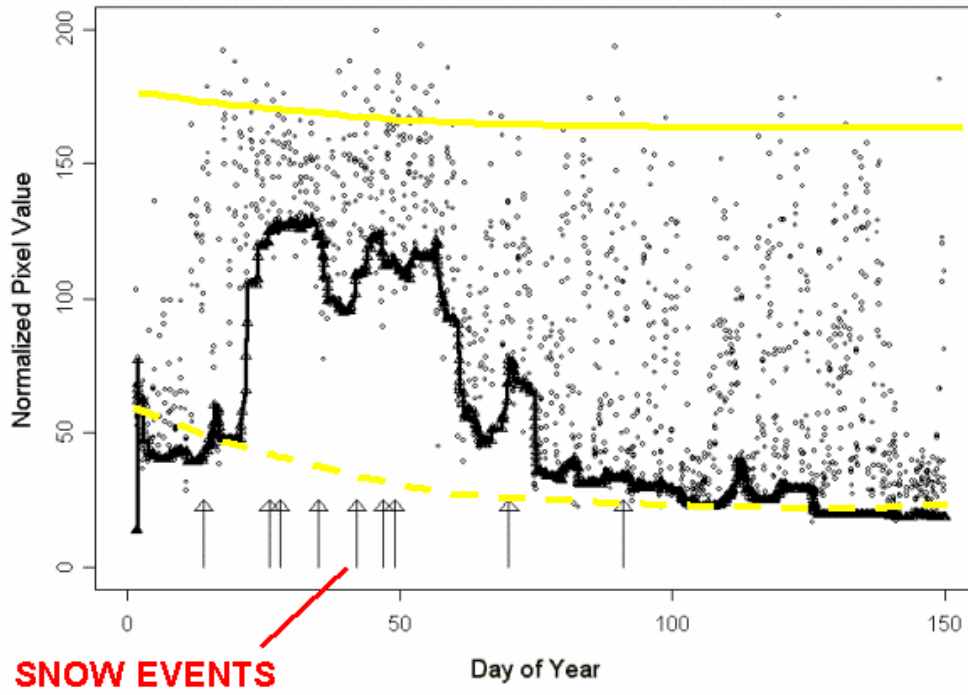


Figure 3

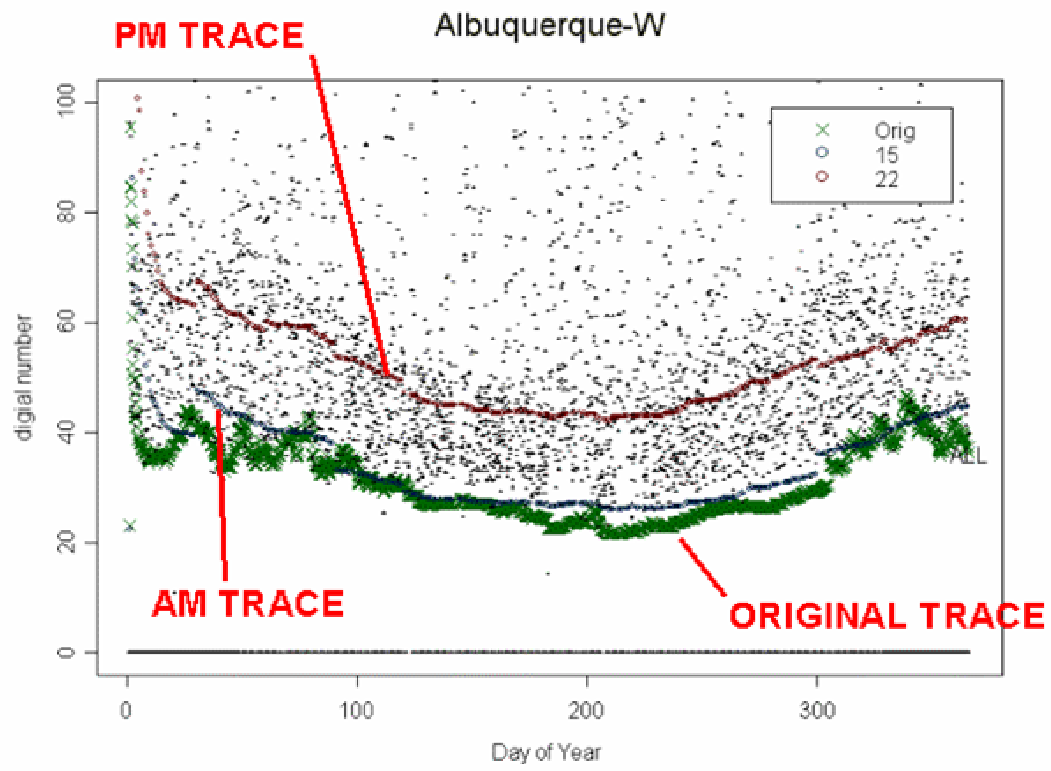


Figure 4

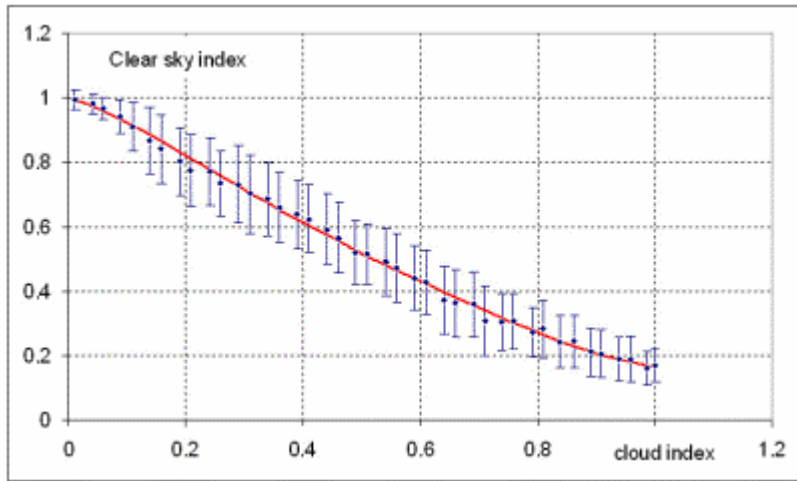


Figure 5

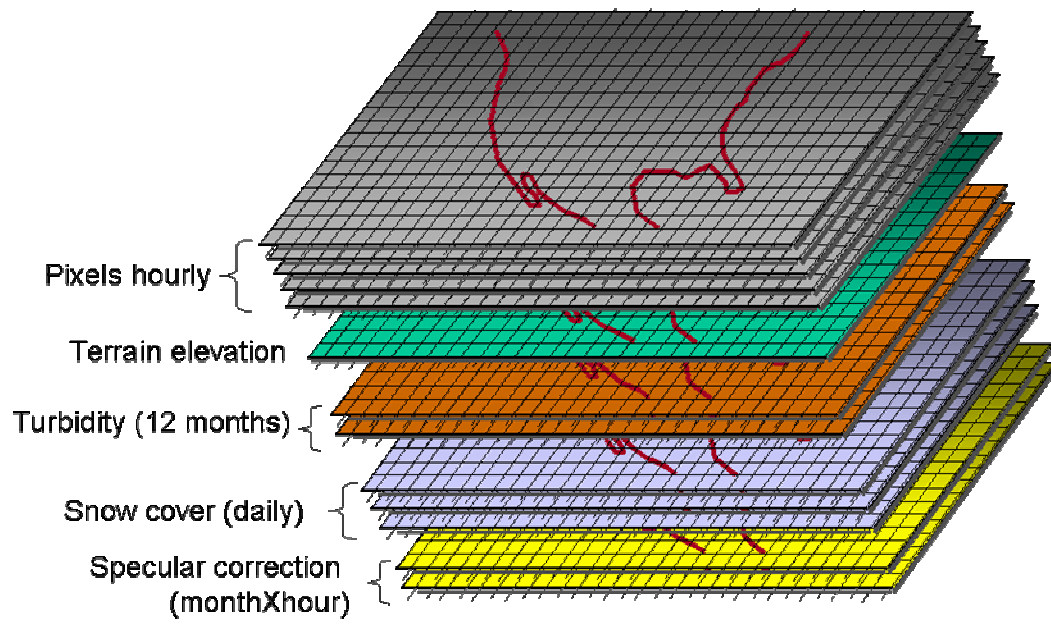


Figure 6

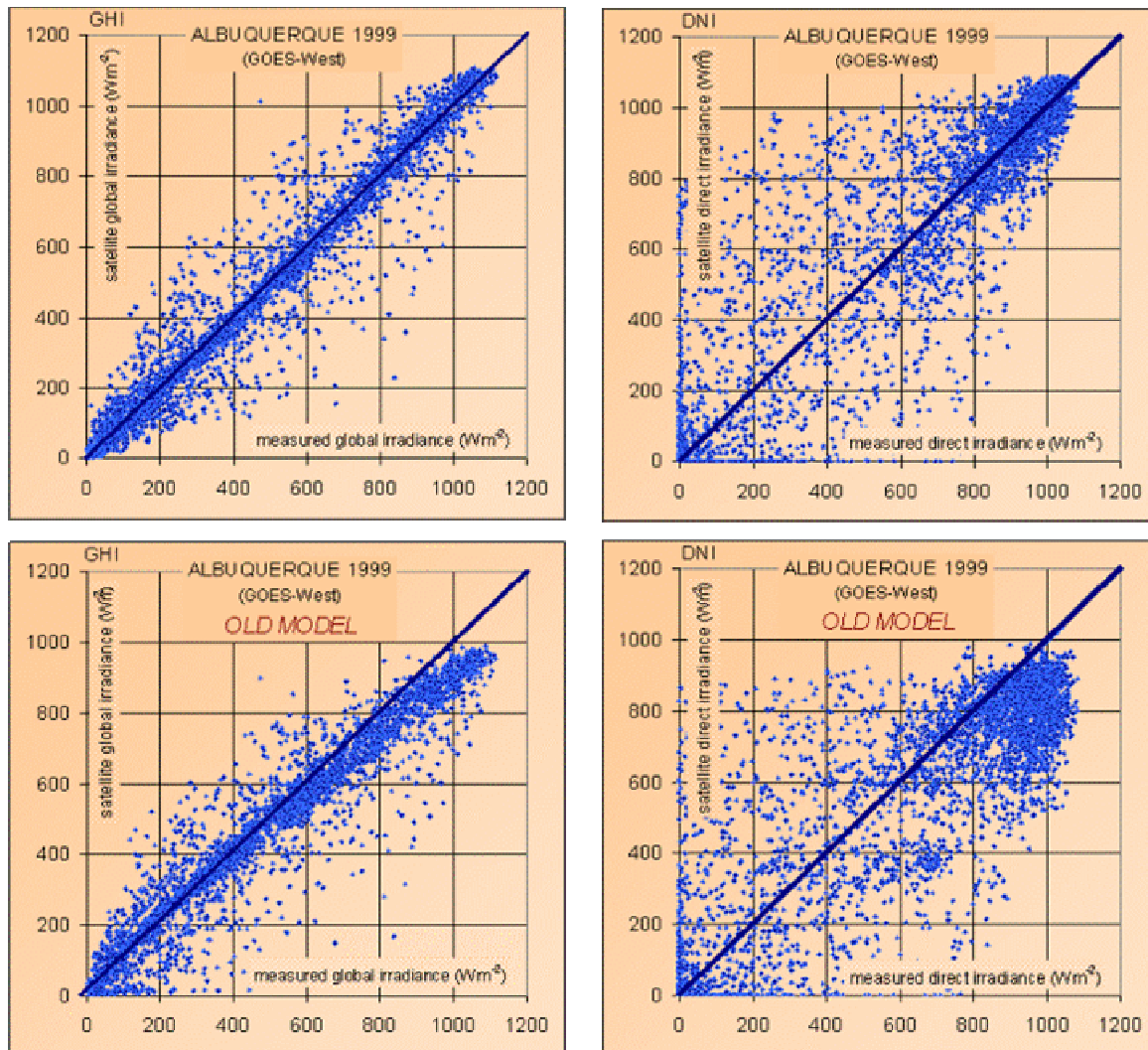


Figure 7

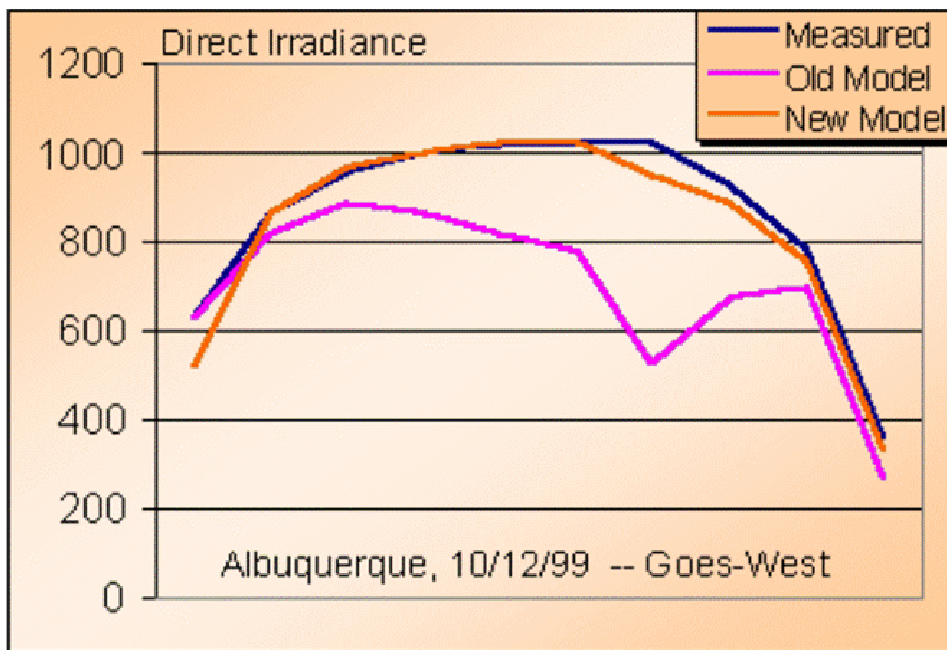


Figure 8

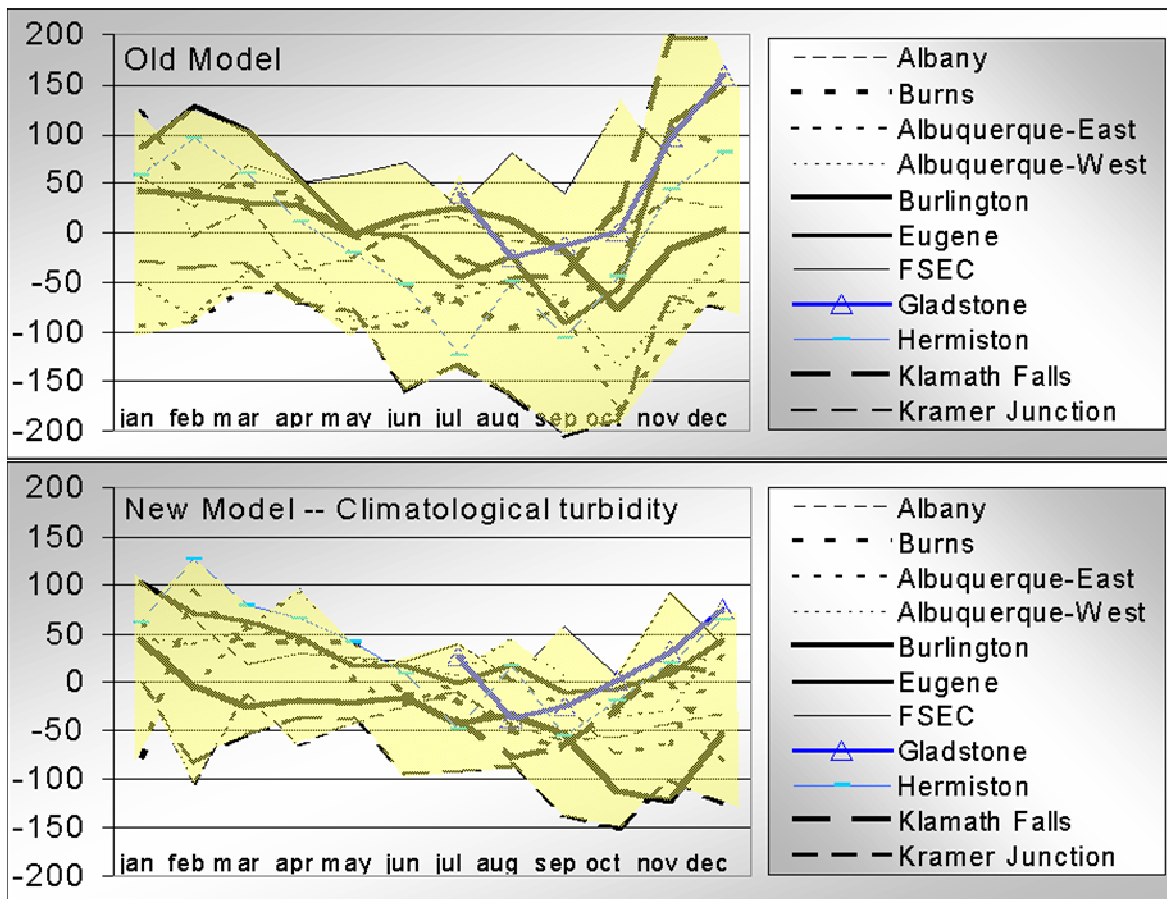


Table 1

Site	Climate	Notes
Albany, NY (1999)	Humid continental	BSRN [ref]
Burns, OR (1999-2000)	Semi-arid, high elev.	Pacific Northwest network
Albuquerque, NM (1999)*	Arid, high elevation	Sandia Natl. Labs, ARM protocol
ARM-Burlington, KS (1999)	Dry continental	ARM –SGP extended facility [ref]
Eugene, OR (1999)	Temperate	Pacific Northwest network
FSEC-Cocoa, FL (1999)	Subtropical	Florida Solar Energy center
Gladstone, OR, (part-1999)	Temperate, humid	Pacific Northwest network
Hermiston, OR (1999-2000)	Temperate, dry	Pacific Northwest network
Klamath Falls, OR (pt-1999)	Temperate dry	Pacific Northwest network
Kramer Junction, CA (1999)	Arid	SEGS power plant monitoring

Picture below

Site	Climate	Notes
Albany, NY (1999)	Humid continental	BSRN [ref]
Burns, OR (1999-2000)	Semi-arid, high elev.	Pacific Northwest network
Albuquerque, NM (1999)*	Arid, high elevation	Sandia Natl. Labs, ARM protocol
ARM-Burlington, KS (1999)	Dry continental	ARM –SGP extended facility [ref]
Eugene, OR (1999)	Temperate	Pacific Northwest network
FSEC-Cocoa, FL (1999)	Subtropical	Florida Solar Energy center
Gladstone, OR, (part-1999)	Temperate, humid	Pacific Northwest network
Hermiston, OR (1999-2000)	Temperate, dry	Pacific Northwest network
Klamath Falls, OR (pt-1999)	Temperate dry	Pacific Northwest network
Kramer Junction, CA (1999)	Arid	SEGS power plant monitoring



Table 2

GLOBAL		RMSE			MBE		
Day-time avg - Wm-2		old	new	new*	old	new	new*
Albany	326	72	68	69	-7	-11	-1
Burns-99	391	89	79	79	-20	-21	-20
Burns-00	383	69	62	62	2	1	2
Albuq. (Goes-E)	485	76	69	69	-31	-3	-5
Albuq. (Goes-W)	486	90	80	80	-22	1	-1
ARM-Burlington	355	57	51	51	6	-1	2
Eugene	311	64	53	53	3	7	4
FSEC-Cocoa	421	121	115	118	34	31	52
Gladstone	290	64	60	60	18	17	24
Hermiston-99	358	52	45	45	-6	2	-2
Hermiston-00	357	47	44	44	7	15	11
Klamath-Falls	357	58	47	50	18	7	16
Kramer Junction	487	69	48	49	-19	-11	8
All sites	385	61	54	64	-4	0	3

DIRECT		RMSE			MBE		
Day-time avg - Wm-2		old	new	new*	old	new	new*
Albany	345	165	154	155	5	-40	-3
Burns-99	483	204	190	188	-33	-41	-35
Burns-00	477	198	172	171	-1	-5	0
Albuq. (Goes-E)	629	179	169	165	-84	-4	-19
Albuq. (Goes-W)	629	205	187	185	-64	26	8
ARM-Burlington	397	131	121	117	5	-42	-28
Eugene	305	158	116	112	18	23	7
FSEC-Cocoa	339	209	193	207	62	36	100
Gladstone	276	151	118	122	38	11	48
Hermiston-99	494	151	133	129	-19	21	2
Hermiston-00	434	163	138	135	-17	25	5
Klamath-Falls	493	199	163	174	33	-17	31
Kramer Junction	672	231	156	161	-104	-83	27
All sites		161	137	137	-19	-11	4

## Appendix A. 2—PRODUCING SATELLITE-DERIVED IRRADIANCES IN COMPLEX ARID TERRAIN

Richard Perez  
ASRC, the University at Albany  
251 Fuller Rd.  
Albany, NY 12203  
[perez@asrc.cestm.albany.edu](mailto:perez@asrc.cestm.albany.edu)

Pierre Ineichen,  
CUEPE, University of Geneva  
7 Route de Drize  
1227 Carouge, Switzerland  
[Pierre.Ineichen@cuepe.unige.ch](mailto:Pierre.Ineichen@cuepe.unige.ch)

Marek Kmiecik, ASRC  
Kathleen Moore, IED  
251 Fuller Rd.  
Albany, NY 12203  
[moore@iedat.com](mailto:moore@iedat.com)

David Renne & Ray George  
NREL  
1617 Cole Blvd.  
Golden, CO 80401  
[drenne / ray\\_george@nrel.nrel.gov](mailto:drenne / ray_george@nrel.nrel.gov)

### ABSTRACT

This paper describes a methodology to correct satellite-derived irradiances over complex terrain for models that use the visible satellite channel as main input for cloud index determination. Complex terrain is characterized by high reflectance surface and or the juxtaposition of high and low reflectance surfaces (e.g., desert plains and forested ridges). The correction consists of (1) climate dependent post-model clear sky calibration and (2) singularity identification and removal.

### 1. DESCRIPTION OF CURRENT MODEL

The authors recently proposed a new semi-empirical model for deriving global and direct irradiances from the visible channel of geostationary weather satellites (Perez et al., 2002). This model was a logical evolution of earlier work by Cano et al., (1986) and Zelenka et al., (1999).

In its simplest description the model amounts to the modulation of clear sky -- global and direct -- envelopes as a function of satellite-derived **cloud indices**. The clear sky envelopes are locally adjustable for regional/seasonal turbidity and ground elevation.

For a given time/location, a cloud index is derived from image's pixel brightness in relation to the local pixel's **dynamic range** -- i.e., the possible range of pixel brightness at the considered location, with the darkest pixels corresponding to clear conditions and the brightest to cloudy conditions. Pixel dynamic range varies as a function of location and time because of ground reflectivity (albedo), ground bi-directional – specular – reflectivity, the presence of snow cover, and the satellite sensor's calibration. In its operational version, the model maintains individual, unique dynamic ranges for all locations. Dynamic ranges evolve over time and are derived from the flux of incoming pixel counts at each location (see Fig. 1). This approach allows the model to dispense with absolute satellite calibration (Perez et al., 2002) and to account for seasonal and geographical changes in ground reflectivity. Further, access to external information on ground snow cover (Perez et al., 2002) allows the model to

also account for snow in its dynamic range management.

Ground specular reflectance had been identified as the main source of model inaccuracy in arid regions. The model addresses the bi-directional reflectance issue by deriving daily/seasonal specular reflectance signatures for each individual location. These signatures are based upon the history of pixel brightness at each considered location, by looking at the variation of observed dynamic ranges' lower bound as a function of day-of-year and time of day (Perez et al., 2002).

## 2. LIMITATIONS OF CURRENT MODEL IN COMPLEX AND/OR ARID TERRAIN

The model was tested against ground truth stations located in the arid western US and was found to perform adequately (Perez et al., 2002). However, these stations, namely, Daggett, CA, Albuquerque, NM and Burns, OR, are not located in extreme ground reflectance environments.

We define extreme ground reflectance environments as

- (1) very high specular regions such as salt beds found throughout the southwestern US and Mexico and in many other arid regions of the world, and/or
- (2) the juxtaposition of bright and dark areas, such as arid plains and forested ridges (see Fig.2)

In the first case, the specular signature imbedded in the current model proved to be sometimes insufficient, leading to small but significant underestimations, particularly noticeable on the direct irradiance (DNI) component. In the second case, slight satellite navigation uncertainties may induce very large errors. Indeed, because location-specific dynamic ranges are maintained by the flux of incoming pixel counts at that location, a satellite navigation error may at times "throw in" dark pixels (from a forested ridge) into otherwise bright ground regions. These few dark pixels reduce the local dynamic range's lower bound, resulting in large model underestimation, because most clear occurrences are mistaken for cloudy conditions when contrasting the clear bright ground pixel against the darker dynamic range. This process is illustrated in Fig. 3.

## 3. PROPOSED SOLUTION

We developed a two-step addition to the model in an attempt to address these shortcomings.

### Step-1: Clear sky calibration

By definition, the lower bound of the dynamic range corresponds to viewing, through a clear sky, a pixel illuminated by clear sky global (GHI) and direct (DNI) irradiances. At some locations, this clear sky limit may not be achieved by the model, because of an underestimated specular signature, or because of the contamination of the lower bound by neighboring darker pixels. In the first case the limit may be reached only at some hours in the day. In the second case, the limit may not be reached at all. In order to force the model to reach this limit, we postulate that for each monthly period, GHI and DNI are bound to reach their clear sky limit at least "n" times for each daylight hour. The value of "n" may be adjusted to reflect prevailing regional insolation conditions. For very clear/arid regions in the SW US, a value in the 5-10 range -- out of 28 to 31 days in a month -- was found to be conservative. This assumption allows us to derive a set of correction coefficients for each pixel, each time-of-day and each month, defined as the ratio between the clear sky (DNI or GHI) value and the n<sup>th</sup> highest achieved value for each hour in the considered monthly period, and thus to produce a calibrated time series.

### Step-2: Removal of singularities

Even after application of the above correction, we found that there remained micro regions of model underestimation. We believe that in these small, highly reflective regions, the model approaches its clear sky limit often enough, because of mis-navigated neighboring darker pixels, so that the clear sky calibration correction is underestimated. These micro-regions errors become visible as singularities when average DNI values are mapped (see Fig. 4). Our approach for this second step correction is to use the average maps themselves as the instrument of data correction. For both the DNI and GHI components, the corrective process scans the monthly average maps in latitude and longitude to detect pixel-to-pixel irradiance variation. If a threshold -- currently set at 2.5% for

monthly average DNI and 1.5% for GHI for two neighboring locations (distant of 10 km) -- is exceeded, the model reduces the singularity by returning an average of the neighboring pixels. In this process, a monthly averaged map without singularities (fig. 4) is constructed. If necessary, time series at the corrected locations may be generated using a secondary model previously developed by the authors (Perez, 2001). This secondary model is designed to simulate a time series of global and direct irradiance from the knowledge of (1) an existing time series – in the present case the uncorrected time series – and (2) the monthly average modified clearness index (Perez et al, 1990) difference between the uncorrected and the corrected monthly maps.

#### 4. DISCUSSION

We have presented a robust, straightforward two-step approach to correct irradiance estimated from weather satellites' visible channel, in cases where terrain reflectivity and texture limit the model ability to perform reliably. The first step – clear sky calibration – typically results in correction of less than 5% for global and less than 10% for direct in bright terrain conditions. The second step may result in higher corrections, but only for a very limited number of pixel locations.

As an alternate approach we are exploring using the IR channel in addition to the visible channel in these difficult locations.

Validation: the initial model had been thoroughly validated for several climatically distinct locations (Perez et al., 2002). Additional validations for this proposed model update are not as straightforward to accomplish, because few ground-truth stations are deployed in problematic micro-regions. However, the NOAA-SURFRAD station of Desert Rock, NV (SUFRAD, 2003) happens to be located in an arid valley with high ground reflectivity and could be used to test the first step of the proposed model modification. Validation results are shown in Fig. 5. They clearly show that the clear-sky calibration brings modeled values much closer to the 1-1 line. The yearly MBEs prior to correction were respectively -4% for global and -11% for direct. After correction, both MBEs are within 1%.

No station was found to operate in micro-structure areas where the step-2 modification would be necessary. However it should be noted, at the very least, the implementation of step-2 provides a means of assessing data quality by gauging the magnitude of the correction applied to any given pixel.

#### 5. ACKNOWLEDGEMENT

This paper is a by-product of research and development efforts funded by the USDOE via University of Oregon (280111A), NREL (DE-AC36-99GO10337 and AXE-0-30070-01) and UNEP (SWERA GF/2721-01-4378).

#### 6. REFERENCES

- (1) Perez R., P. Ineichen, K. Moore, M. Kmiecik, C. Chain, R. George and F. Vignola, (2002): A new operational model for satellite-derived irradiances description and validation. *Solar Energy* (in press).
- (2) Cano, D., J.M. Monget, M. Aubuisson, H. Guillard, N. Regas and L. Wald, (1986): A Method for the Determination of Global Solar Radiation from Meteorological Satellite Data. *Solar Energy* 37, pp. 31-39
- (3) Zelenka, A., Perez R, Seals R. and Renné D., (1999): Effective Accuracy of Satellite-derived irradiance, *Theoretical and Applied Climatology*, 62, 199-207
- (4) Perez, (2001): A time Series Generator. Technical Report No. 3. NREL contract AXE-0-30070-01. NREL, Golden, CO.
- (5) Perez, R., P. Ineichen, R. Seals and A. Zelenka, (1990): Making Full Use of the Clearness Index for Parameterizing Hourly Insolation Conditions. *Solar Energy* 45, pp. 111-1
- (6) The SURFRAD Network -- Monitoring Surface Radiation in the Continental United States. NOAA, Surface Radiation Research Branch (<http://www.srrb.noaa.gov/surfrad/index.html>)

## Figure titles

Fig 1: Evolution of dynamic range at a sample location. Each dot represents a pixel count corrected for solar incidence. The upper bound reflects the decay of satellite calibration. The lower bound reflects seasonal variability of ground albedo. Both upper and lower bounds are derived from the history of pixel count at that location.

Fig. 2: Satellite view of the southwest US showing complex ground reflectivity. Two extreme cases – salt beds – are shown by arrows. One of these salt beds is shown on the right as seen from an airplane at 10 km elevation.

Fig. 3: Illustration of dynamic ranges for two neighboring pixels near Death-Valley, California. One of the pixels (A) has a dark albedo and the other (B) a high ground albedo (see satellite scene top left). Routine satellite navigation uncertainties result in an artificial decrease of the apparent pixel B's lower bound, because pixel A values are sometime recorded in pixel B location. As a consequence, pixel B appears considerably cloudier than pixel A, leading to irradiance underestimation at that location.

Fig. 4: Comparing uncorrected and corrected (both step-1 and step-2) monthly averaged direct irradiance maps in a 400 x 400 km region straddling California and Nevada (average  $\text{Wm}^{-2}$ ). Note that the overall upper trend is largely due to implementation of step-1, while the elimination of singularities is a result of step-2.

Fig. 5: Satellite estimated vs. ground truth measurements at Desert Rock, NV, for global irradiance before and after step-1 correction (respectively A and B) and direct irradiance before and after step-1 correction (respectively C and D)

Figure 1

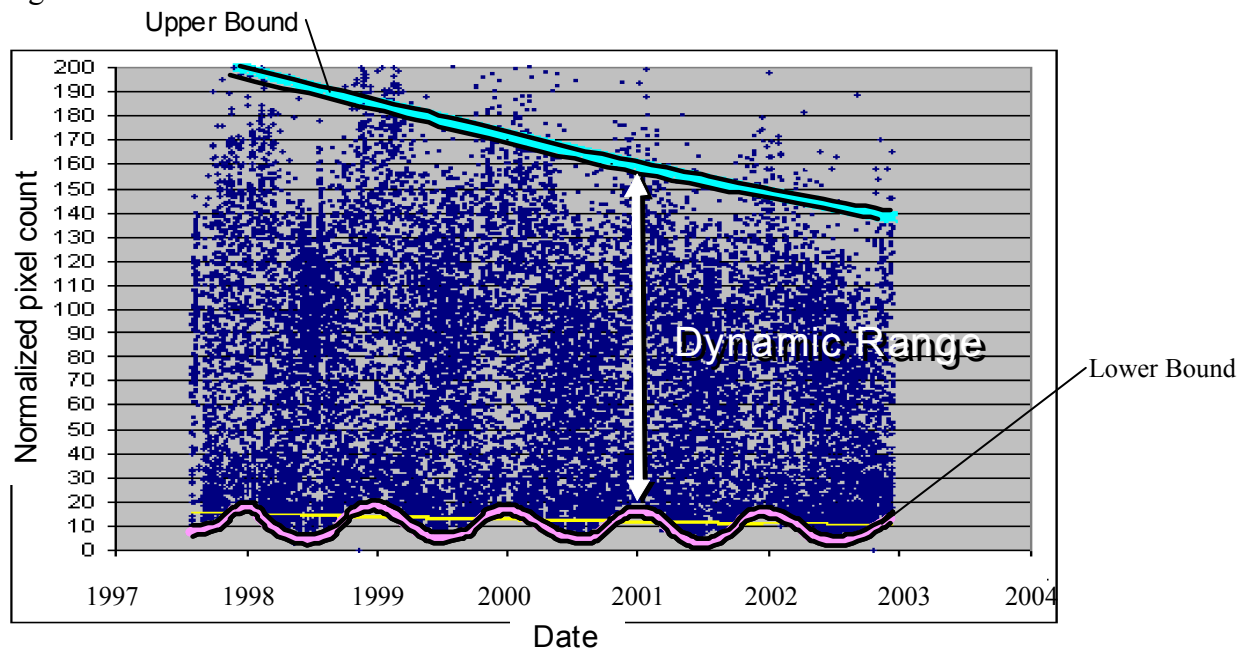


FIGURE 2



FIGURE 3

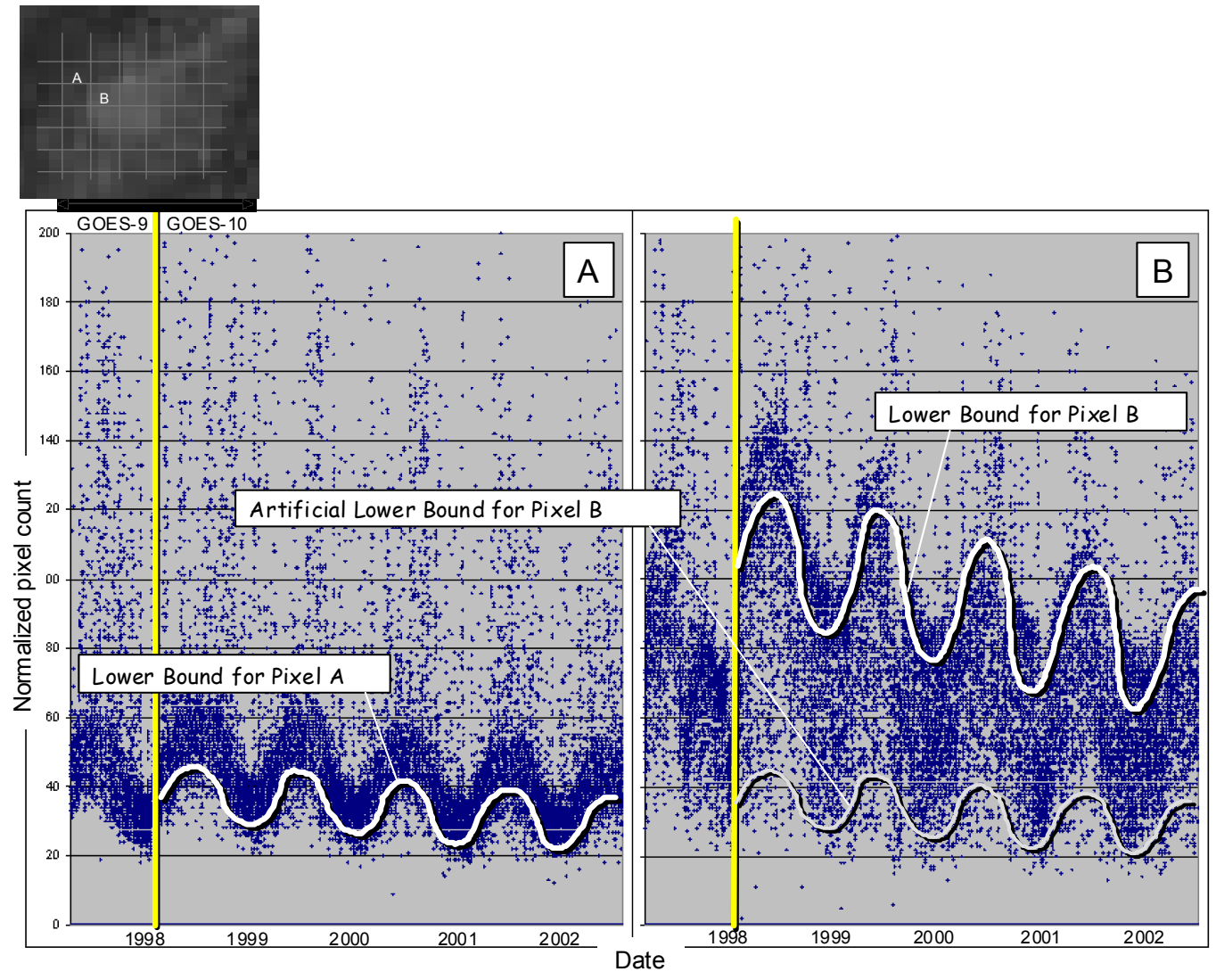




FIGURE 4

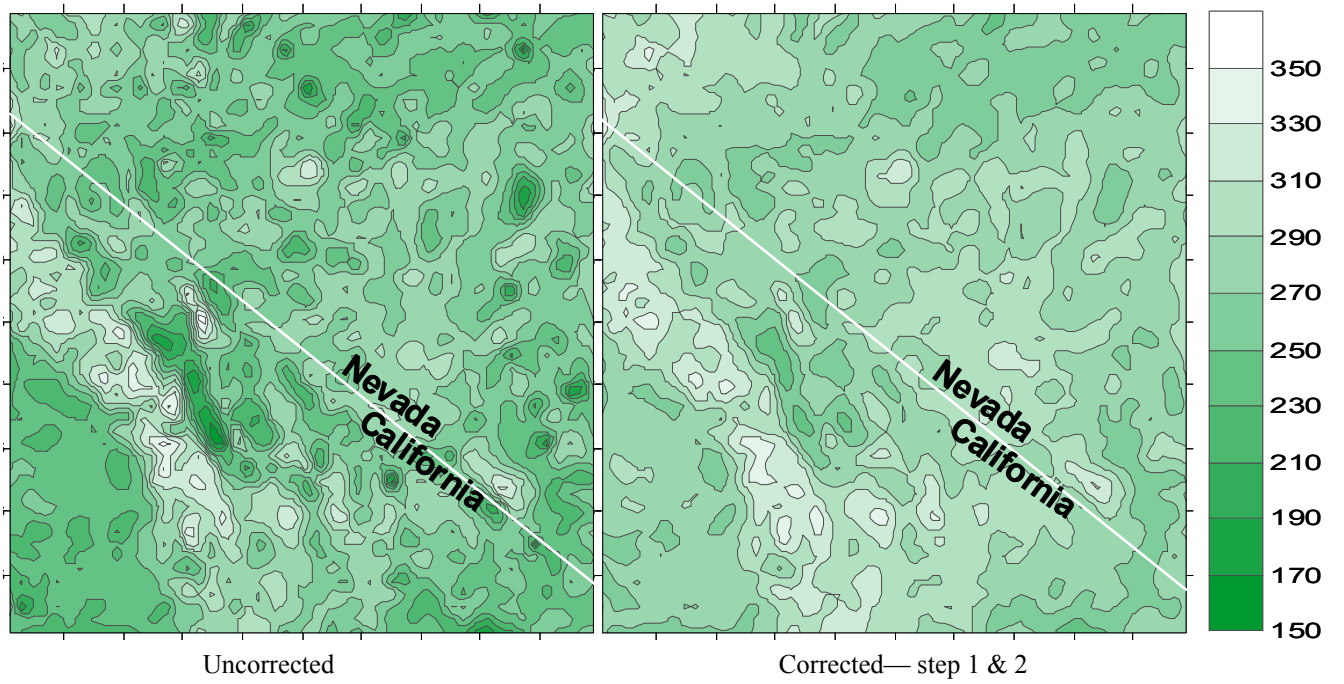
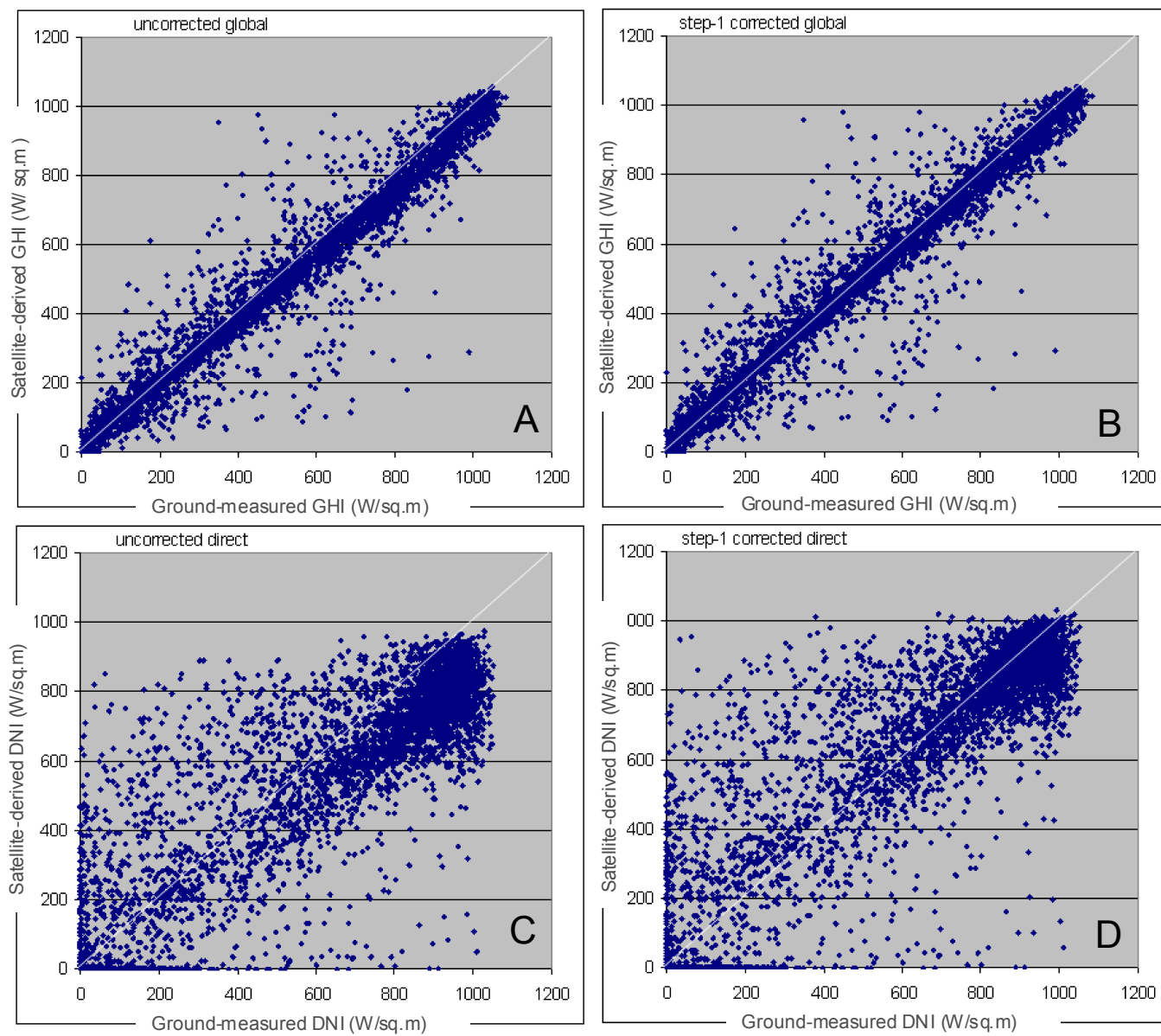


FIGURE 5



# Appendix B—Solar Calculator Information

University of Oregon  
Solar Radiation Monitoring Laboratory

## UO SRML Solar Calculator Help

### Table of Contents

[Introduction](#)

[About this program release \(v 2.1\)](#)

[System requirements](#)

[Installation](#)

[Uninstalling the Calculator](#)

[A useful tip](#)

[The Main tab](#)

[Choosing a station profile](#)

[Selecting algorithms](#)

[Computing with averaged time values](#)

[About data file column names](#)

[The Run button](#)

[The Return to Excel button](#)

[The Help button and context-sensitive help](#)

[The Station profile tab](#)

[Basic station profile parameters](#)

[Selecting a source for air pressure](#)

[Selecting a source for temperature](#)

[Selecting a source for wind speed](#)

[Selecting a source for year](#)

[Creating a new station profile](#)

[Deleting a station profile](#)

[The Profile \(part 2\) tab](#)

[Entering tilt parameters](#)

[Entering PV array parameters](#)

[Selecting sources for irradiance data](#)

[Selecting a source for albedo](#)

[The Preferences tab](#)

[Setting station and algorithm preferences](#)

[Setting the Calculator window size](#)

[Types of calculations](#)

[Data file format requirements](#)

[SRML numeric data element codes](#)

[SRML data quality flags](#)

[SRML station ID codes](#)

## Introduction

The Solar Calculator add-in for Microsoft Excel is a program that operates closely with Excel to provide a variety of functions concerning solar irradiance and other matters related the position of the sun. This program was developed by the University of Oregon Solar Radiation Monitoring Laboratory (UO SRML). The solar position calculation is based on the SOLPOS program—written by the National Renewable Energy Laboratory (NREL)—which, in turn, is based on algorithms first published by Joe Michalsky. In addition, calculations of PV power output and related data are based on NREL's PVWATTS software, which incorporates a PV performance model developed at Sandia National Laboratories. For information about obtaining the SRML Solar Calculator software, please contact us.

### About this program release (v. 2.1)

This release of the Solar Calculator contains some features which are not yet fully functional. Two of the calculations, **Beam from global irradiance** and **Beam from tilted irradiance**, are still in an experimental stage. These are algorithms that model direct normal (beam) irradiance based on other types of irradiance inputs. Further research is needed to improve these models so that they are as useful as possible. Nevertheless, they may be of interest to some even at this preliminary stage. A future release of the Calculator will improve upon them.

### System requirements

The Calculator has been tested with the following Microsoft operating systems: **Windows XP**, **Windows 2000 Professional**, **Windows NT Workstation 4.0**, and **Windows 98**. It is known to work with **Microsoft Excel XP**, **Excel 2000**, and **Excel 97**. The program *may* be compatible with certain other system configurations, but these have not been tested by the UO SRML.

It is recommended that your computer have a Web browser installed on it so that you can conveniently view this help file while using the Calculator. Either **Netscape Navigator** or **Microsoft Internet Explorer** is compatible. You can use any other browser to read this file, but the Calculator will not be able to launch it automatically. Please note that you do *not* need to have an Internet connection to your computer: except for a few links, this help file is self-contained and it resides on your local computer.

Installation of the Solar Calculator will result in the creation of a folder called **C:\SRML** on your computer, and the total disk space used will be about 1 megabyte (1 MB). No changes will be made to the Windows Registry database.

There are no other specific system requirements, but as always, when running an application that does a great deal of computation, you are best served by a computer with a fast processor and lots of RAM.

### Installation

If you have not already installed the Solar Calculator, and you have an installation diskette or CD-ROM, here is the procedure:

- **Exit** from Excel, if it is currently running.
- Insert the installation diskette in drive A: or B:, or insert the CD-ROM in your computer's CD-ROM drive.
- Execute a file, on the diskette or CD-ROM, called **Install.xls**. You can do this by clicking on the file name in **Windows Explorer**, or by accessing the **Run ...** option on the Windows **Start** menu, typing the file name, and pressing the **Enter** key.
- If you are unable to execute the file as described above, then start up Excel as you normally would, and open the Install.xls file.

Follow any further directions displayed on your screen. If you do not have an installation diskette or CD-ROM, or if your computer does not have a floppy disk drive or CD-ROM drive, it is still possible to install the Calculator. Please contact us for assistance.

### Uninstalling the Calculator

It's simple to uninstall the Calculator: (1) Remove **Solar Calculator** from Excel's list of Add-Ins, and (2) delete the **C:\SRML** folder. You can do this in the reverse order, but then Excel will display an error message on your screen.

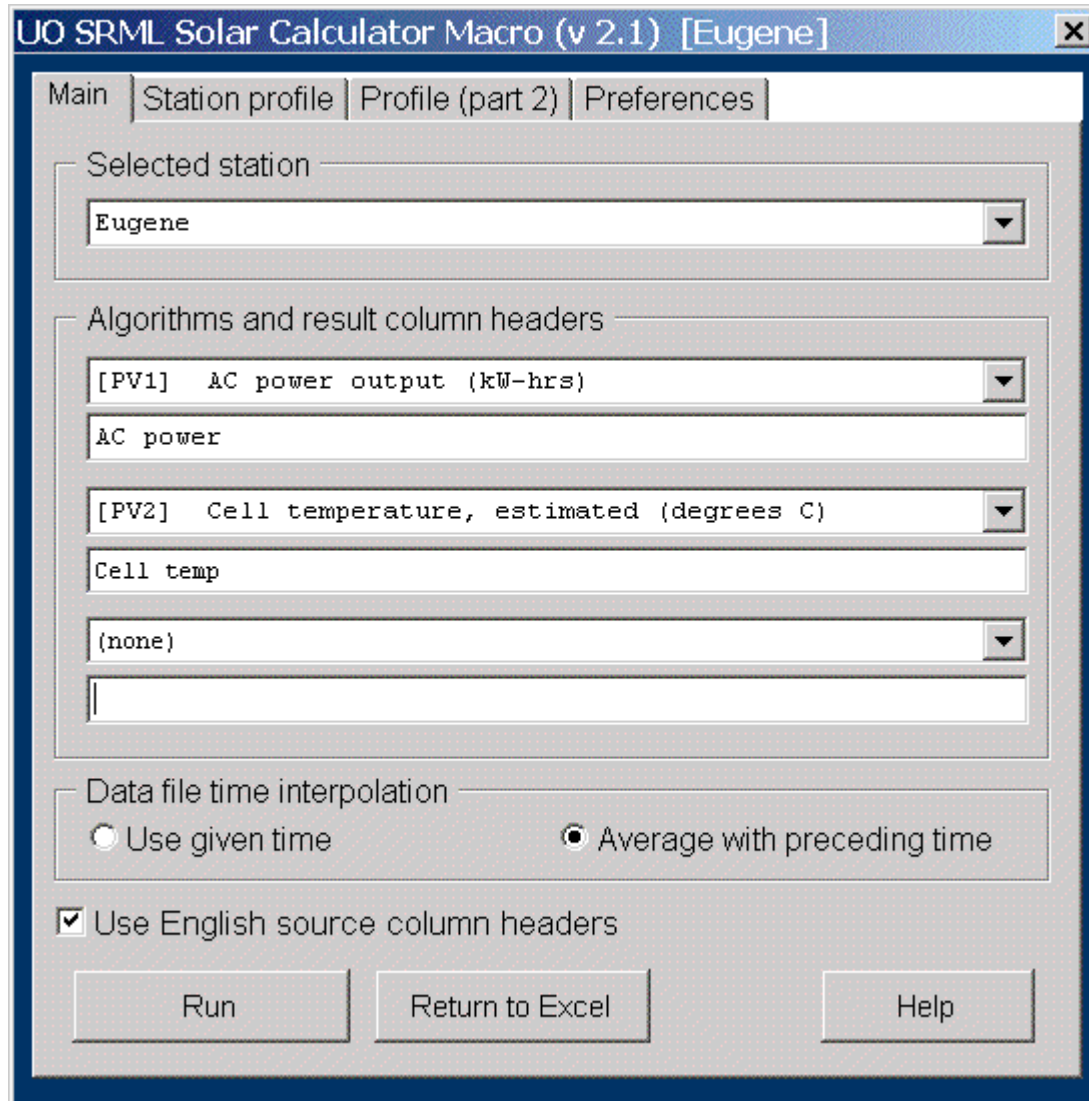
### A useful tip

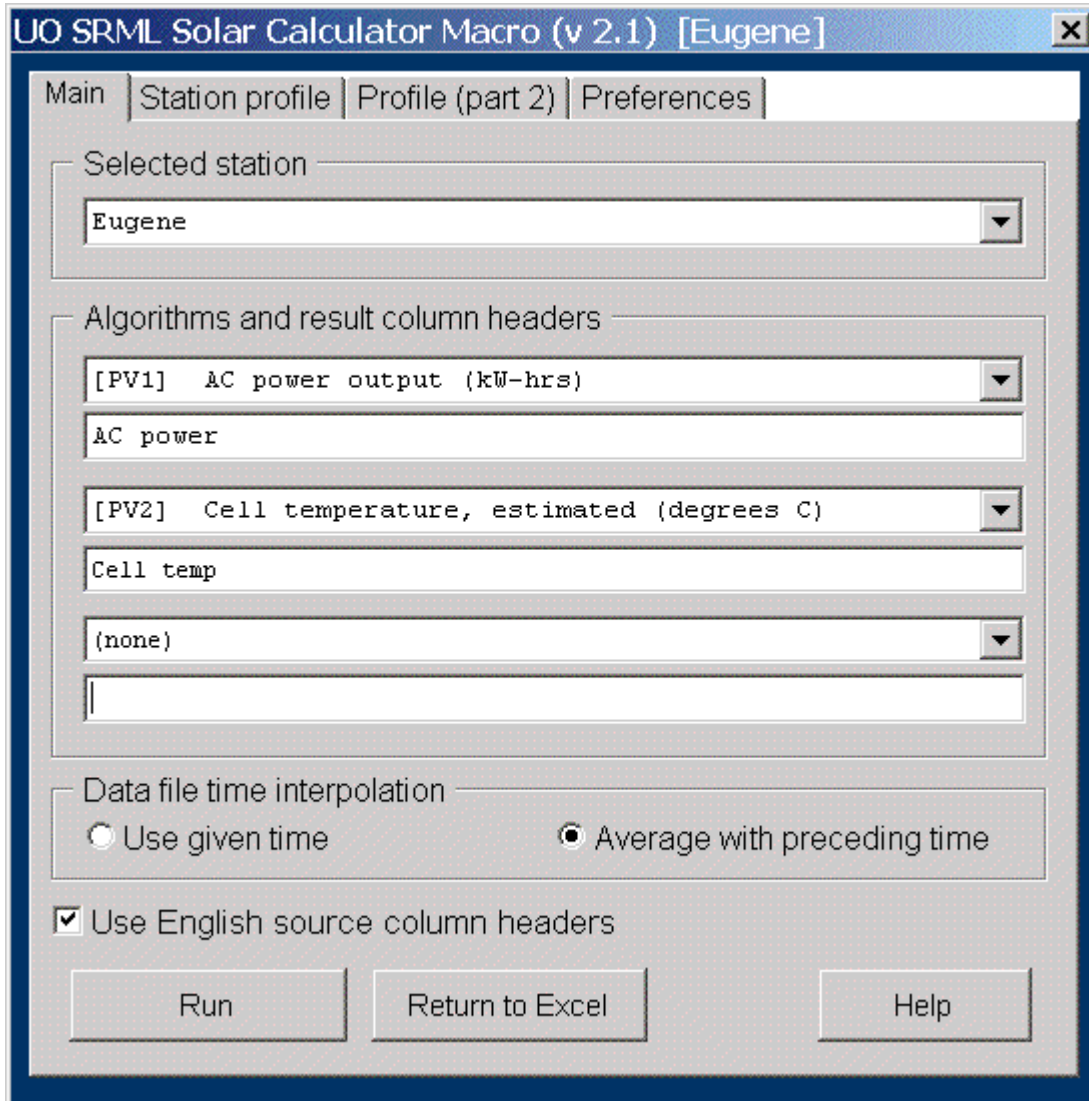
**Note: whenever you make a change to a setting, it takes effect at once, and it is in effect the next time you use the program.** There is no need to explicitly *save* your work, since this is done for you automatically. This behavior may differ from that of other programs you've used. The Solar Calculator was designed to be easy to use effectively, and it does not interrupt your thought process to ask if you really mean what you're saying. In reality, though, nothing too drastic can happen. With one exception, the Calculator cannot ever delete or change

existing data in your worksheet. Please note, however, that **your worksheet's header row *may* be altered** by the Calculator. Otherwise, the only things that can change are the particular settings you've indicated you want to use with the Calculator. And, as you'll see, it's very easy to create these. The remainder of this help file is devoted to the details of working with the Calculator.

#### The Main tab

This is the screen you see when the Solar Calculator starts up. Here, you select the program settings to use—these are called **station profiles**—and which algorithms to employ. It is here that you actually run the Solar Calculator. Detailed information about these and additional features follow the example screen below.





### Choosing a station profile

Station profiles are sets of program parameters that you can create, edit, and delete. Here is where you choose the particular profile to use for the calculations you want to perform. When the Calculator starts up, it attempts to find a station profile that is appropriate for the data in your active worksheet. However, you can override this behavior by selecting a profile from the drop-down list.

When you first install the Solar Calculator, the list contains a number of such station profiles, most of which correspond to monitoring stations where we collect solar radiation data. (In addition, there may be some profiles that are meant to be used with TMY2 data.) Using other features of this software, you can tailor the list to suit your own purposes. In particular, you can create multiple station profiles for selected monitoring stations, and each of these profiles can specify parameters that alter, in some respect, the Calculator's behavior.

Note that there is one profile, the **Default Station** profile, which does not represent a real monitoring station. This set of parameters merely exists so that you'll always have at least one *template* to use when creating new profiles. Most of the parameters for this profile can be edited, although the profile itself cannot be deleted.

### Selecting algorithms

The Solar Calculator can perform from one to three calculations simultaneously. Each calculation uses one of about fifty distinct algorithms which you can choose using the three algorithm list boxes on the **Main** tab. Many of these algorithms yield results deriving from the position of the earth at given times, while others also involve figuring the degree of refraction of the atmosphere, the amount of solar irradiance under various conditions, or PV power output.

In the above screen example, you can see that the two selected calculations have descriptive names preceded by short designations in square brackets. Each of these codes consists of a category (**PV**, **RAD**, **GEOM**, or **XTRA**), followed by a number. They are intended to help you navigate more quickly through the drop-down lists of calculations.

In the PV category are algorithms closely related to PV, or photovoltaic, applications. The RAD category consists of other algorithms that concern solar irradiance. GEOM is a large category that groups algorithms that have to do with computing the apparent position of the sun. Finally, XTRA is a collection of algorithms that do not fit in the other three categories, or that are probably not as commonly used as the others. As you'll see when we discuss the **Preferences** tab, there is another program feature to help you organize this list of algorithms (and the list of station profiles).

Besides choosing particular algorithms, you can also specify the header text that Excel will display, respectively, in each corresponding result column of your worksheet. Initially, these column headers are set to the (long) names of each of the various algorithms. You'll probably want to shorten them considerably. The above example screen depicts customized column headers.

While the Calculator is limited to three calculations at a time, you can perform more by simply repeating the process of choosing algorithms and clicking the **Run** button.

For your convenience, any selected algorithms and edited column headers are remembered for you as part of the station profile you're currently using.

#### [Computing with averaged time values versus given time values](#)

This program feature may be confusing at first, but it is quite useful. For example, when computing the solar irradiance on a tilted surface, you may be using a data file that contains global, diffuse, and direct normal (beam) measurements *averaged* over a particular time interval—typically 5, 15, or 60 minutes. However, the time values that are given in the data file generally represent the ending boundaries of these intervals. So, using times mid-way between each of the given points in the data file will more accurately model the circumstances in which such irradiance measurements are valid. In such cases, you should select the **Average with preceding times** option.

On the other hand, if you select the **Use given time** option, all computations will be done as if the inputs (solar irradiance values, air pressure, etc.) are those that were in effect at the exact times found in the data file. This option is perfectly valid if you are generating results that have to do only with the earth's position at a given time, and not with any other measured, averaged input data.

For your convenience, the option you choose here is remembered for you as part of the station profile you're currently using.

#### [About data file column names](#)

Near the bottom of the Main tab is a check-box labeled **Use English source column headers**. When a check mark appears in this box (the default setting), you'll notice that certain worksheet column headers consist of descriptive English words, abbreviations and numbers. In addition, you'll find that the same sorts of names occur in various drop-down list boxes on the Calculator form. These names will usually suffice to convey the actual *type* of data found in corresponding worksheet columns.

Normally, you should leave this program feature in its default state. If you click the box to remove the check mark, all the mnemonic names (in the worksheet and in the Calculator form) will be replaced by 4-digit numbers. These numbers are used at the UO Solar Radiation Monitoring Lab when processing data files automatically. No harm should come from repeatedly clicking this check-box. However, keep in mind that the format that is active when you quit the Calculator will be in effect for your data file.

#### [The Run button](#)

The Run button does just what you'd expect: it causes the Calculator to perform the calculations you've selected. However, prior to this, your active Excel worksheet is checked for data that might cause problems during the calculations. As well, the options and parameters you've specified on the Calculator form are checked for consistency and completeness. Consequently, just after clicking this button, you may see a message on the screen informing you of a potential problem that needs to be addressed before the calculations can take place.

#### [The Return to Excel button](#)

Clicking the **Return to Excel** button closes the Calculator program and allows you to perform any other Excel functions you choose.

Unfortunately, you cannot access your worksheet or any general features of Excel while the Calculator is running. This is characteristic of all Excel add-in applications that are compatible with Excel 97. However, you may quit the Calculator at any time, and when you next run it, you'll find that all the settings are just as you left them.

#### [The Help button and context-sensitive help](#)

Clicking the **Help** button causes your Web browser to open this help document. Notice that this button appears on each tab, or page, of the Calculator's form. The particular section of this file that you'll see first depends on the Calculator tab that is active when you click the button. Please note that *context-sensitive* help is available for nearly all features of the Calculator program. To use it, position your mouse cursor on a feature, then *right-click* to see the **What's this?** menu item nearby. Click this menu item to navigate directly to documentation in this file that concerns the program feature you've selected.

#### The Station profile tab

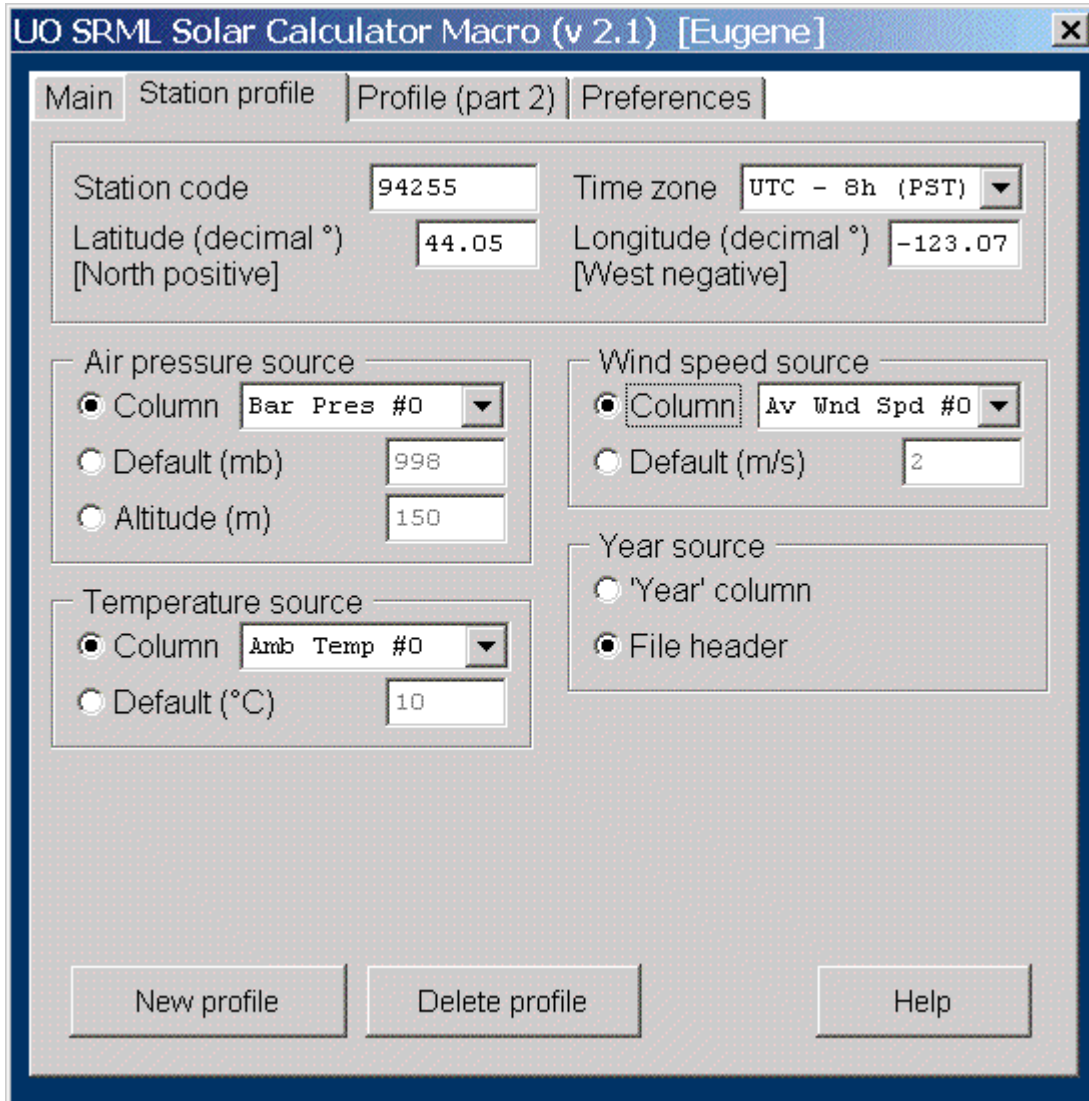
This screen contains the basic parameter settings that define a station profile, including its location and information about certain data file columns. This is where some of the customizing of station profiles is done, and it's where you can create new ones or delete unneeded ones. Detailed information concerning features on this tab follows the example screen below.

The screenshot shows a software window titled "UO SRML Solar Calculator Macro (v 2.1) [Eugene]". The window has four tabs: "Main", "Station profile", "Profile (part 2)", and "Preferences". The "Station profile" tab is selected. The interface is organized into several sections:

- Station code:** 94255
- Latitude (decimal °) [North positive]:** 44.05
- Longitude (decimal °) [West negative]:** -123.07
- Time zone:** UTC - 8h (PST)
- Air pressure source:**
  - Column: Bar Pres #0
  - Default (mb): 998
  - Altitude (m): 150
- Wind speed source:**
  - Column: Av Wnd Spd #0
  - Default (m/s): 2
- Temperature source:**
  - Column: Amb Temp #0
  - Default (°C): 10
- Year source:**
  - 'Year' column
  - File header

At the bottom of the window, there are three buttons: "New profile", "Delete profile", and "Help".





#### Basic station profile parameters

At the top of the screen, there is a set of four important parameter settings: **Latitude**, **Longitude**, **Time zone**, and **Station code**. Latitude and longitude are in (decimal) degrees, with southern latitudes and western longitudes expressed as negative values. Time zones are negative offsets from Universal Time Code (UTC) west of Greenwich. If you have incorrect values in any of these fields, the Calculator will not generate the results you desire.

The station code is, by the UO SRML convention, a 5-digit number that corresponds to a particular physical monitoring station. In the National Solar Radiation Data Base, these values correspond to WBAN numbers. Such codes also occur in our data files, and the Calculator uses the code value to determine which station profile to load initially. Specifically, the Calculator loads the profile that is **first in alphabetical order** among any whose station code matches the one in the worksheet. If no match is found, the **Default Station** profile is loaded. We have included a [list of these codes](#) near the end of this help document.

#### Selecting a source for air pressure

Air pressure is one of the inputs to about a dozen algorithms which involve atmospheric refraction. As you can see, there are several ways to specify it: as actual measured data values (in millibars) in a particular worksheet column, as a default value in millibars, or as a derived value that is calculated from altitude in meters. The default value is also used whenever an air pressure value in the worksheet is bad (flagged "99").

#### Selecting a source for temperature

Temperature is another input that is used for calculating refraction. It also has an effect on PV performance

calculations. It can be read from a given column (of Celsius data) in the Excel worksheet. Alternatively, it can be specified as a default Celsius value. The default value is also used whenever a temperature value in the worksheet is bad (flagged "99").

#### Selecting a source for wind speed

Like some of the other settings, wind speed can be specified as a default value, or as data to be gotten from a particular worksheet column. Wind speed, which should be in meters per second, is used by the Calculator in modeling the performance of PV cells. If the wind speed value in a particular row of your worksheet is bad (flagged "99"), then the default value is assumed.

#### Selecting a source for year

The Solar Calculator always needs specific dates and times to determine the location of the sun—or, according to Copernicus, the earth. These values are taken from the first two columns of your active Excel worksheet. However, the year portion of the date is normally found in the second column of the worksheet header, in which case it is *global* to the worksheet, understood to be the year in which all dates and times occur. For all typical UO SRML data files, you should then specify the **File header** option.

In the case of worksheet data we derive from TMY2 files, each month block of data values may occur in a different year. Consequently, the Calculator cannot apply a single year value to the entire worksheet; instead, the year must be in a column of its own. For TMY2 data, you should select the **'Year' column** option. Note: If **Use English source column headers** is not checked (active) on the **Main** tab, this option will read **'8888' column**. If you have questions about using TMY2 data with the Solar Calculator, please contact us.

#### Creating a new station profile

The way to create a new station profile is to copy an existing one, then edit the copy. Choose a profile that is most like the one you want to create, then click the **New profile** button. You'll be asked to enter a name for the new profile, and this must be unique. You may find it helpful to choose a name corresponding to the specific parameter settings in the profile. For example, you might incorporate the tilt angle or an irradiance column header in the name.

**Important:** Remember that any changes you make to a profile take place immediately. Therefore, unless you really want to edit an existing profile, you should click the **New profile** button first, editing only the new copy.

#### Deleting a station profile

When you click the **Delete profile** button, **the currently loaded profile is immediately deleted**. The Calculator then attempts to find another profile whose station code matches the one in your Excel worksheet. If more than one exists, it will load the one that is next, alphabetically; if none exist, it will load the **Default Station** profile.

The **Delete profile** function is provided so that you can dispose of experimental profiles or those that are just used temporarily. However, the Calculator allows you to have as many profiles as you want—well, tens of thousands, anyhow. Consequently, you really don't need to delete any of them. As you'll see further below, there is another way to avoid having to select a profile from a very crowded list.

#### The Profile (part 2) tab

This screen supplements the **Station profile** tab with parameter settings that are required for real-world applications of solar irradiance data. At present, such uses involve PV array performance and modeling of direct normal (beam) irradiance. In the future, the Calculator may support other application areas, such as daylighting and solar water heating. Detailed information concerning features on this tab follows the example screen below.

UO SRML Solar Calculator Macro (v 2.1) [Eugene]

Main | Station profile | Profile (part 2) | Preferences

Tilted surface settings

Tilt (decimal °) 41

Aspect (decimal °) 180

PV array settings

Array type fixed

AC Rating (kW) 5

DC Rating (kW) 5

DC/AC conversion efficiency (0 to 1) 0.85

Power cost (¢/kWh) 6.8

Irradiance

Derive tilted irradiance

Global Global #0

Beam Beam #0

Diffuse Diffuse #1

Use tilted measurements

Column Tilt180 45 #0

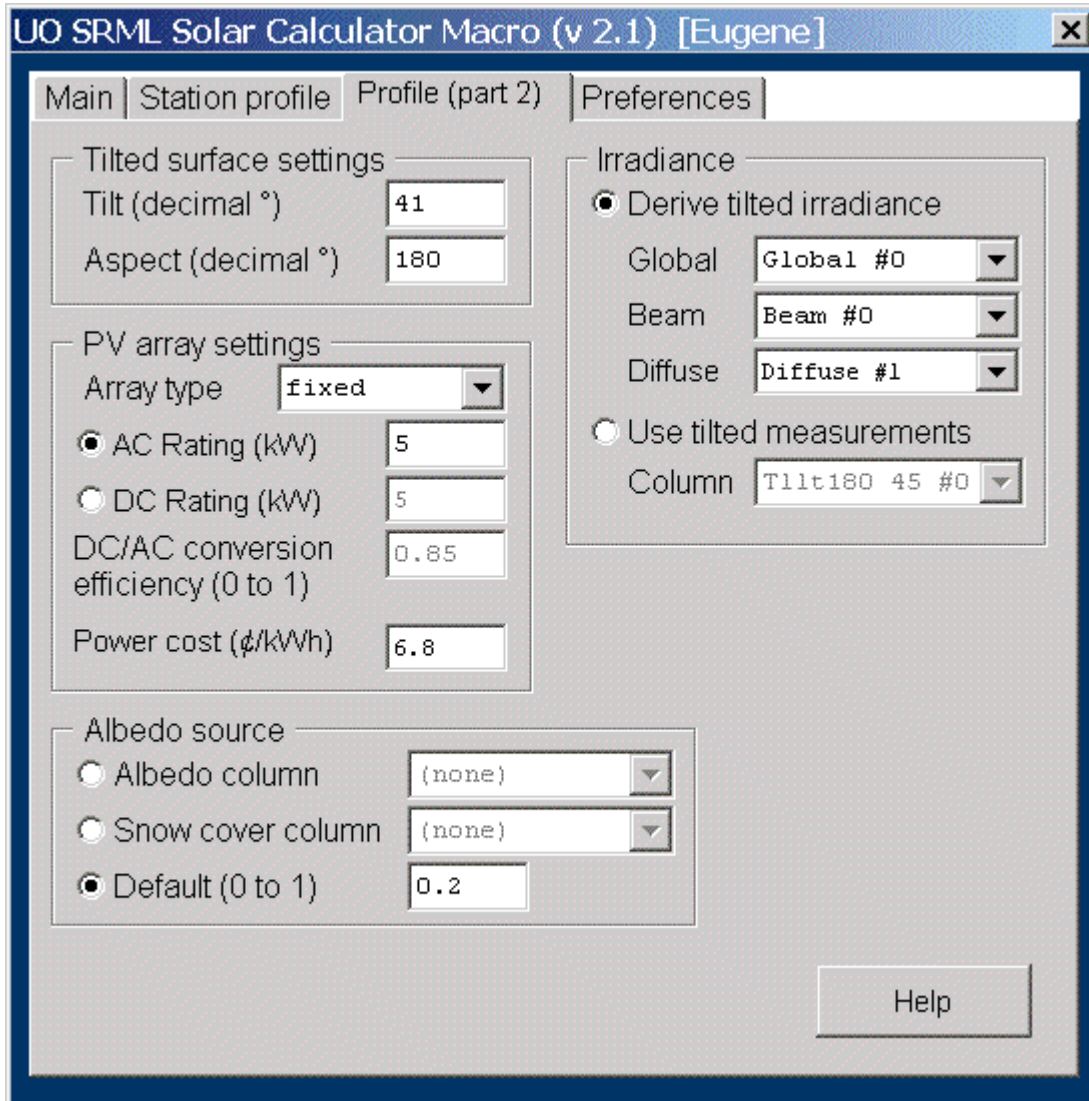
Albedo source

Albedo column (none)

Snow cover column (none)

Default (0 to 1) 0.2

Help



#### Entering tilt parameters

Tilt, in degrees, describes the angle formed by a surface with respect to the plane that is tangent to the earth's surface at its location. Aspect, also in degrees, describes the direction of the tilted surface, with zero being due north, 90 due east, 180 due south, and 270 due west.

**Note: tilt and aspect settings here must agree with those implied for any measured tilted irradiance values** specified on the right side of this tab. In other words, if you set **Tilt** to 30° and **Aspect** to 180°, the selected tilted irradiance column (if any) in the list under the **Use tilted measurements** option must contain data that have been measured by a device with this same tilt and aspect. Failure to insure this consistency will lead to erroneous results.

#### Entering PV array parameters

Obviously, PV array settings are used for modeling the output of PV arrays. There are three types of arrays to choose among: **fixed**, **1-axis**, and **2-axis**. In addition, you specify the power rating of the array, and, to see how much money might be saved (on electric bills, at least), you can specify the energy cost in cents per kilowatt-hour. There are two ways to specify the PV power rating. Either give its **AC Rating**, or provide both the **DC Rating** and **DC/AC conversion efficiency**.

**Note: Tilted surface settings must specify the tilt and orientation (aspect) of the array.** In case you are modeling multiple arrays of various power ratings and tilts, you can break the calculations up into stages and then, using normal Excel functionality, sum the individual array results.

#### Selecting sources for irradiance data

The Calculator requires irradiance inputs for certain calculations. Here you can specify, first, whether actual tilted

irradiance data should be used, or whether the Calculator should derive or model tilted irradiance based on global horizontal, direct normal, and diffuse input values. Once you select one of the options **Derive tilted irradiance** or **Use tilted measurements**, you must then select the actual column or columns in your worksheet that contain these data.

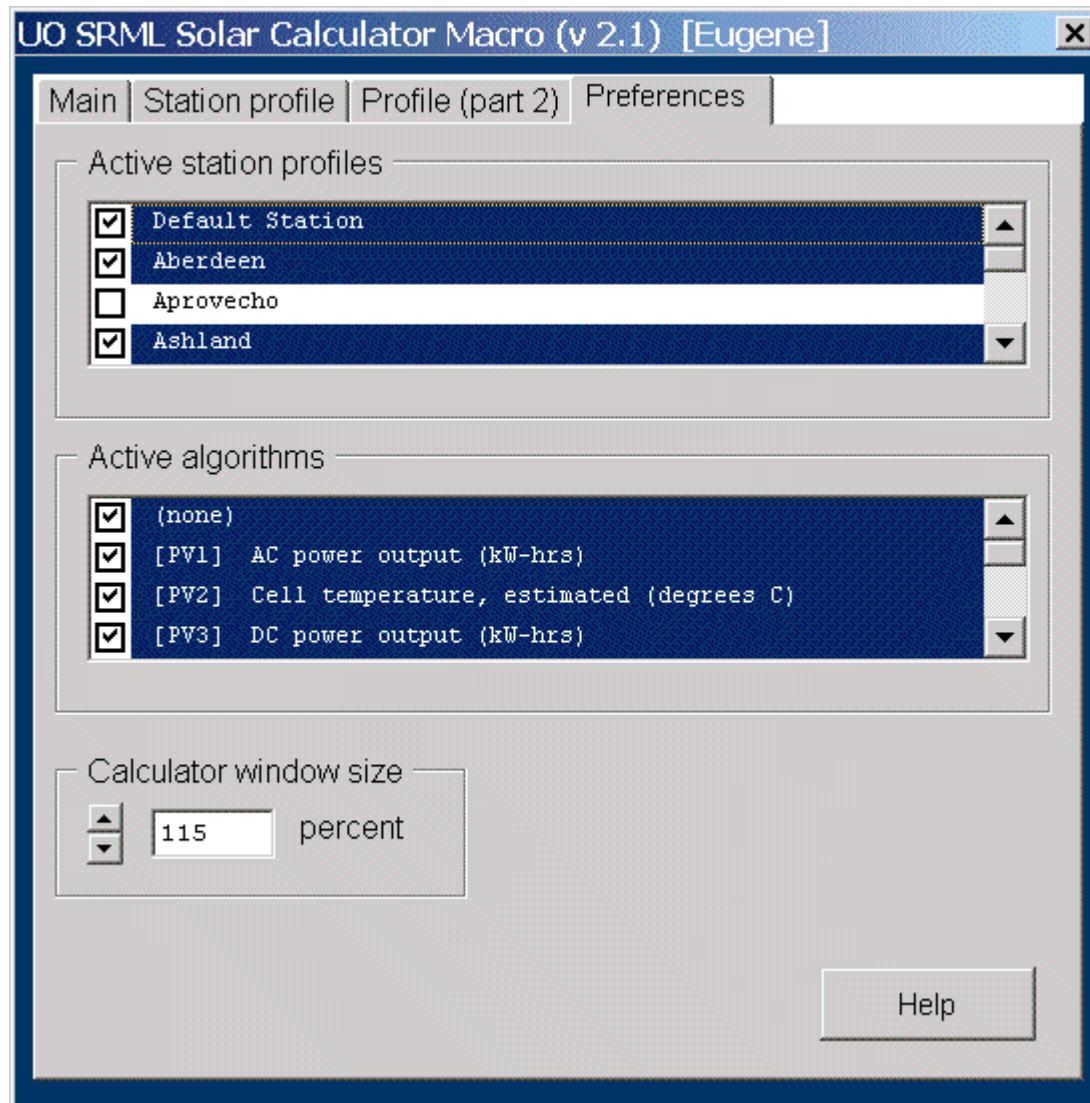
Although you can specify any of the list values, calculations using irradiance data will not be performed unless corresponding columns actually exist in your active Excel worksheet. The Calculator only checks for this at the moment you click the **Run** button, so you can configure settings for station profiles that will not be used immediately. (This is also true of all columns you select on the **Station profile** tab.)

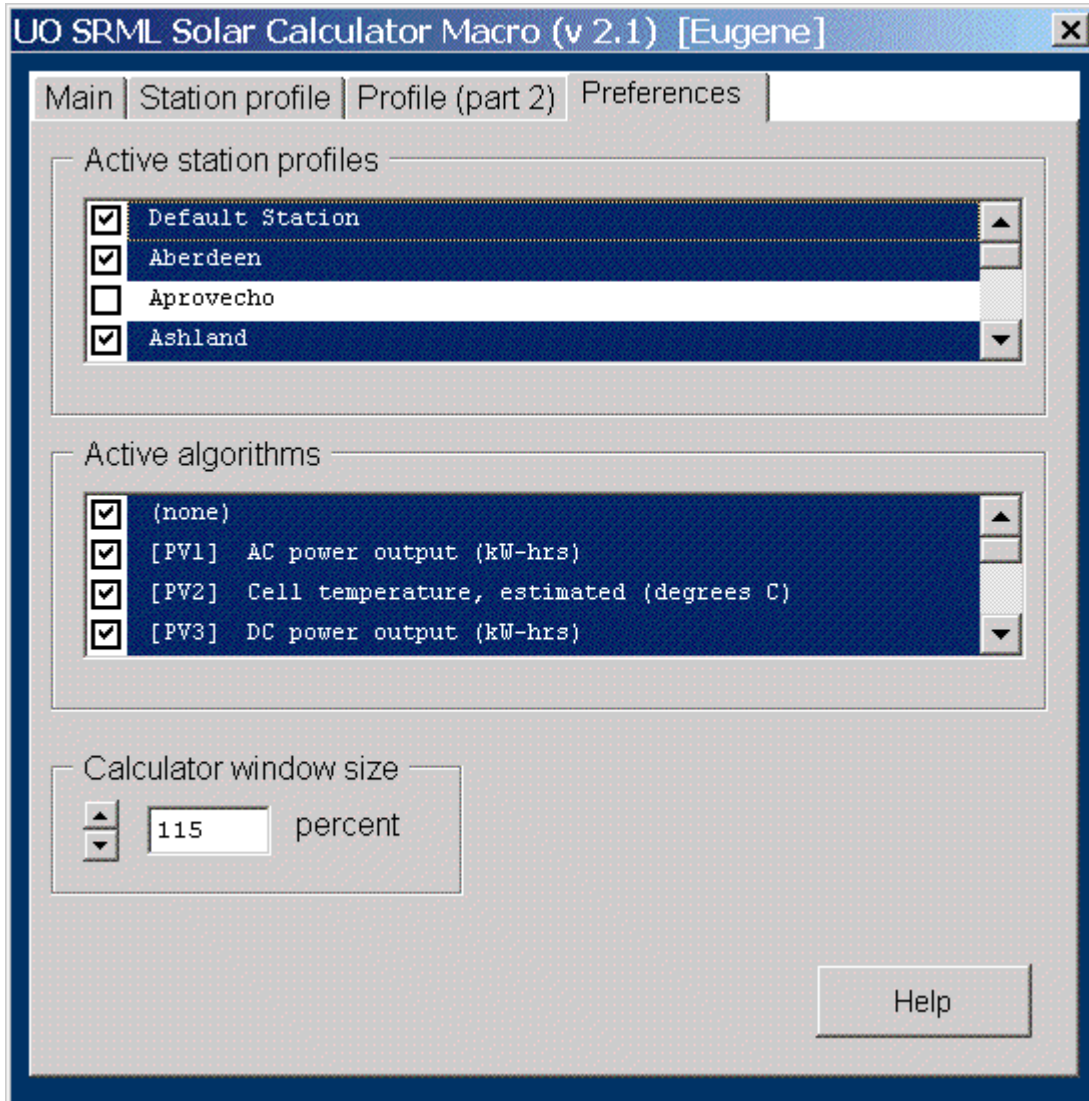
#### Selecting a source for albedo

Albedo, or ground reflectivity, is only used by the Calculator to model tilted irradiance. Note that the second option, **Snow cover column**, should be selected if your worksheet contains TMY2 data. The **Default** option should be used if neither measured albedo nor snow cover data are available. A value of 0.2 is typically assumed for the types of calculations this software performs.

#### The Preferences tab

This screen contains features that do not pertain to a single station profile, but are more global in scope. Here you can determine which station profiles and which algorithms you want to see in the selection lists on the **Main** tab. As well, you can set the size of the Solar Calculator screen to best match your monitor's dimensions and pixel resolution.





#### Setting station and algorithm preferences

The two lists provide a means to specify which station profiles and which algorithm types will be *active*; i.e., selectable in the pull-down lists on the **Main** tab. This is fairly straight-forward, but there is one side-effect that should be noted: **Only active station profiles are loaded automatically**. This allows you to determine which profile—among possibly several having identical station codes— gets loaded when a particular station code appears in your Excel worksheet. Otherwise, it is always the one that is first in alphabetical order.

#### Setting the Calculator window size

Use this feature to adjust the Calculator's window size so that you can comfortably read all the text and manipulate all the controls. Clicking the up-arrow increases the window size; clicking the down arrow decreases it. The size percentage relative to a default setting is displayed to the right of these arrows. You cannot directly enter a percent value in the text box. Note that, due to the way Excel deals with screen fonts, some size settings will result in truncated labels or unintentional boldface text. If you experiment a bit with different settings, you'll be able to find one that works for your computer. Like all the Calculator's settings, your choice of window size is remembered for you until you change it.

#### Types of calculations

Each of the currently provided algorithm types are listed below:

- [PV1] AC power output (kW-hrs)
- [PV2] Cell temperature, estimated (degrees C)

- [PV3] DC power output (kW-hrs)
- [PV4] Irrad. transmitted to PV module (W-hrs/m<sup>2</sup>/hr)
- [PV5] Value of AC power (cents)
- [RAD1] Shadow-band correction factor
- [RAD2] Tilted irrad., isotropic diffuse model (W-hrs/m<sup>2</sup>/hr)
- [RAD3] Tilted irrad., Perez diffuse model (W-hrs/m<sup>2</sup>/hr)
- [RAD4] Beam from global irrad. (W-hrs/m<sup>2</sup>/hr)
- [RAD5] Beam from tilted irrad. (W-hrs/m<sup>2</sup>/hr)
- [RAD6] Clearness index
- [RAD7] Tilted clearness index
- [RAD8] ET direct normal irrad. (W-hrs/m<sup>2</sup>/hr)
- [RAD9] ET global horizontal irrad. (W-hrs/m<sup>2</sup>/hr)
- [RAD10] ET total irrad., tilted surface (W-hrs/m<sup>2</sup>/hr)
- [RAD11] Prime
- [RAD12] Unprime
- [GEOM1] Air mass, relative optical
- [GEOM2] Air mass, pressure-corrected
- [GEOM3] Azimuth angle, solar (degrees)
- [GEOM4] Declination (degrees north)
- [GEOM5] Earth radius factor
- [GEOM6] Elevation angle, refracted (degrees)
- [GEOM7] Equation of time (minutes)
- [GEOM8] Hour angle (degrees west)
- [GEOM9] Incident angle, tilted surface (degrees)
- [GEOM10] Incident angle, cosine of
- [GEOM11] Sunset/sunrise hour angle (degrees)
- [GEOM12] Local sunrise time (minutes from midnight)
- [GEOM13] Local sunset time (minutes from midnight)
- [GEOM14] True solar time (minutes from midnight)
- [GEOM15] True solar time minus local standard time (minutes)
- [GEOM16] Zenith angle (degrees)
- [GEOM17] Zenith angle, refracted (degrees)
- [GEOM18] Zenith angle, cosine of
- [GEOM19] Zenith angle, refracted, cosine of
- [XTRA1] Day angle (degrees)
- [XTRA2] Ecliptic longitude (degrees)
- [XTRA3] Greenwich mean sidereal time (hours)
- [XTRA4] Julian day (days)
- [XTRA5] Local mean sidereal time (degrees)
- [XTRA6] Obliquity of ecliptic (degrees)
- [XTRA7] Mean anomaly (degrees)
- [XTRA8] Mean longitude (degrees)
- [XTRA9] Right ascension (degrees)

- [XTRA10] Time of ecliptic calculations (days)
  - [XTRA11] Universal (Greenwich) Standard Time (hrs)
- [Data file format requirements](#)

This brief discussion will refer to the graphic example directly below. In the example, we see one of the UO SRML's data files—a Eugene 5-minute data file.

Microsoft Excel - EUPF0311.TXT

File Edit View Insert Format Tools Data Window Help SRML

A1 = 94255

	A	B	C	D	E	F	G	H	I	J	K	L	
1	94255	2003	Global #0	0	Beam #0	0	Global #2	0	Global #3	0	Global #8	0	Glob
2	305	5	0	12	0	12	0	12	0	12	0	12	
3	305	10	0	12	0	12	0	12	0	12	0	12	
4	305	15	0	12	0	12	0	12	0	12	0	12	
5	305	20	0	12	0	12	0	12	0	12	0	12	
6	305	25	0	12	0	12	0	12	0	12	0	12	
7	305	30	0	12	0	12	0	12	0	12	0	12	
8	305	35	0	12	0	12	0	12	0	12	0	12	
9	305	40	0	12	0	12	0	12	0	12	0	12	
10	305	45	0	12	0	12	0	12	0	12	0	12	
11	305	50	0	12	0	12	0	12	0	12	0	12	
12	305	55	0	12	0	12	0	12	0	12	0	12	
13	305	100	0	12	0	12	0	12	0	12	0	12	
14	305	105	0	12	0	12	0	12	0	12	0	12	
15	305	110	0	12	0	12	0	12	0	12	0	12	
16	305	115	0	12	0	12	0	12	0	12	0	12	
17	305	120	0	12	0	12	0	12	0	12	0	12	
18	305	125	0	12	0	12	0	12	0	12	0	12	
19	305	130	0	12	0	12	0	12	0	12	0	12	
20	305	135	0	12	0	12	0	12	0	12	0	12	
21	305	140	0	12	0	12	0	12	0	12	0	12	
22	305	145	0	12	0	12	0	12	0	12	0	12	
23	305	150	0	12	0	12	0	12	0	12	0	12	
24	305	155	0	12	0	12	0	12	0	12	0	12	
25	305	200	0	12	0	12	0	12	0	12	0	12	
26	305	205	0	12	0	12	0	12	0	12	0	12	



Microsoft Excel - EUPF0311.TXT

File Edit View Insert Format Tools Data Window Help SRML

A1 = 94255

	A	B	C	D	E	F	G	H	I	J	K	L	M
1	94255	2003	Global #0	0	Beam #0	0	Global #2	0	Global #3	0	Global #8	0	Glob
2	305	5	0	12	0	12	0	12	0	12	0	12	
3	305	10	0	12	0	12	0	12	0	12	0	12	
4	305	15	0	12	0	12	0	12	0	12	0	12	
5	305	20	0	12	0	12	0	12	0	12	0	12	
6	305	25	0	12	0	12	0	12	0	12	0	12	
7	305	30	0	12	0	12	0	12	0	12	0	12	
8	305	35	0	12	0	12	0	12	0	12	0	12	
9	305	40	0	12	0	12	0	12	0	12	0	12	
10	305	45	0	12	0	12	0	12	0	12	0	12	
11	305	50	0	12	0	12	0	12	0	12	0	12	
12	305	55	0	12	0	12	0	12	0	12	0	12	
13	305	100	0	12	0	12	0	12	0	12	0	12	
14	305	105	0	12	0	12	0	12	0	12	0	12	
15	305	110	0	12	0	12	0	12	0	12	0	12	
16	305	115	0	12	0	12	0	12	0	12	0	12	
17	305	120	0	12	0	12	0	12	0	12	0	12	
18	305	125	0	12	0	12	0	12	0	12	0	12	
19	305	130	0	12	0	12	0	12	0	12	0	12	
20	305	135	0	12	0	12	0	12	0	12	0	12	
21	305	140	0	12	0	12	0	12	0	12	0	12	
22	305	145	0	12	0	12	0	12	0	12	0	12	
23	305	150	0	12	0	12	0	12	0	12	0	12	
24	305	155	0	12	0	12	0	12	0	12	0	12	
25	305	200	0	12	0	12	0	12	0	12	0	12	
26	305	205	0	12	0	12	0	12	0	12	0	12	

In the header row of the worksheet, there are several points to note: the **station code** appears in cell A1, the year in cell B1, and succeeding columns alternately contain a **data type code** or the character zero. The latter indicates that the column contains a **data quality flag**. (The UO SRML Web site contains documentation about [station codes](#), [data element numbers](#), and [quality flags](#).)

Data quality flags are used by the Solar Calculator, for certain computations, to determine whether to base calculations on actual data from worksheet columns, or on default values either specified in the station profile or furnished by the Calculator. Default values are used when flags indicate that respective data is unreliable. Note that when the Calculator computes certain new values (such as direct normal irradiance), it also generates an additional corresponding flag column with values pertaining to the resulting calculation.

The example worksheet shows a number of columns for irradiance data: several for global and one for direct normal (beam). In addition, we see that column A contains the yearday, and column B specifies the time. Time is specified in the 24-hour format where 100 is 1:00 am, and 2400 is midnight. This example shows only the left-most columns of the file; other columns that are not visible here contain diffuse irradiance data and various meteorological data.

The Calculator handles data files having the most commonly used time intervals: 5-minute, 15-minute, and hourly. Prior to executing the algorithms you select, the dates and times are checked for validity and consistency. If there is a time or date gap (or a repeated date and time) in your worksheet, the Calculator will notify you with a warning that results may be incorrect. Note, however, that in TMY2 data files, there will usually be at least one such gap or repeated interval. But, because any discontinuities occur at midnight in these files, calculations concerning PV

performance are unaffected.

If you only need to compute certain geometrical results, such as sunrise and sunset times, you could use a worksheet containing just two columns, with the station code and year in the header row, and yeardays and times below.

#### [SRML numeric data element codes](#)

If you are working with files from our Web site, and you do not have the **Use English column headers** option checked on the Calculator's **Main** tab, your Excel worksheet's header row and the contents of various drop-down list boxes on the Calculator form will appear as 4-digit data element codes. The tables below list these codes along with short descriptions.

Solar radiation data  
 First three digits indicate data type  
 Fourth digit differentiates duplicate types

1st	2nd	3rd
0 — Voltage output of solar cell array (millivolts)		
	2 — Tilted 25 degrees	
		4 — West-facing
		6 — South-facing
		8 — East-facing
	3 — Tilted 30 degrees	
		6 — South-facing
	5 — Tilted 45 degrees	
		6 — South-facing
	6 — Tilted 60 degrees	
		6 — South-facing
1 — Global and total solar radiation (watt hours per square meter per hour)		
	0 — Horizontal	
		0 — Horizontal
		9 — Ground-facing
	1 — Tilted 15 degrees	
		6 — South-facing
	2 — Tilted 25 degrees	
		4 — West-facing
		5 — Southwest-facing
		6 — South-facing
		8 — East-facing
	3 — Tilted 30 degrees	
		6 — South-facing
	5 — Tilted 45 degrees	
		6 — South-facing
	6 — Tilted 60 degrees	
		6 — South-facing
	9 — Tilted 90 degrees	
		2 — North-facing
		6 — South-facing
2 — Direct solar radiation (watt hours per square meter per hour)		
	0 — Beam	
		1 — Normal incident
3 — Diffuse solar radiation (watt hours per square meter per hour)		
	0 — Horizontal	
		0 — Horizontal
4 — Current output of solar cell array (milliamper hours per hour)		
	2 — Tilted 25 degrees	
		4 — West-facing
		6 — South-facing
		8 — East-facing
	3 — Tilted 30 degrees	
		6 — South-facing
	5 — Tilted 45 degrees	
		6 — South-facing
	6 — Tilted 60 degrees	
		6 — South-facing
5 — Power output of solar cell array (watts)		
	1 — Tilted 15 degrees	
		6 — South-facing
	2 — Tilted 25 degrees	
		6 — South-facing
	3 — Tilted 30 degrees	
		6 — South-facing
	6 — Tilted 60 degrees	
		6 — South-facing

Spectral solar radiation data All four digits indicate data type				
1st	2nd	3rd	4th	
7 — Spectral data (watt hours per square meter per hour, except for illuminance values which are kilolux hours per hour)				
	0 — Horizontal			
		0 — Horizontal		
			0 — OG 570	
			1 — RG 630	
			2 — RG 695	
			3 — UVA	
			5 — Zenith illuminance	
			6 — Diffuse illuminance	
			7 — Global illuminance	
			8 — Maximum illuminance	
			9 — Minimum illuminance	
	0 — Beam			
		1 — Normal incident		
			0 — OG 570	
			1 — RG 630	
			2 — RG 695	
			3 — UVA	
			7 — Beam illuminance	
			8 — Maximum illuminance	
			9 — Minimum illuminance	

Meteorological data First three digits indicate data type Fourth digit differentiates duplicate types	
1st	2nd and 3rd
9 — Meteorological data	
	10 — Sky condition
	11 — Ceiling height (meters)
	12 — Visibility (kilometers)
	13 — Weather (10-digit code)
	15 — Total rainfall (inches)
	17 — Barometric pressure (millibars)
	20 — Average wind direction (degrees)
	21 — Average wind speed (meters per second)
	22 — Standard deviation of wind direction
	30 — Ambient temperature (degrees Celsius)
	31 — Dew point temperature (degrees Celsius)
	33 — Relative humidity (percent)
	37 — Solar cell temperature (degrees Celsius)
	40 — Average barometric pressure (millibars)
	51 — Total sky cover (10ths of sky dome)
	52 — Opaque sky cover (10ths of sky dome)
	53 — Precipitable water (millimeters)
	54 — Aerosol optical depth
	55 — Snow depth (centimeters)
	56 — Albedo
	65 — Days since last snowfall

### SRML data quality flags

Data quality flags accompany most of the data columns in SRML files. These appear in columns directly to the right of the actual data to which they correspond, and they have the number zero in their header row. They are used for quality control, and to indicate whether, or how, the data were processed. The following table provides an explanation for each of our two-digit flags:

First digit	Second digit
1 — Observed data	
	1 — Raw data
	2 — Processed data
	3 — <a href="#">Possible problems in data</a>
	8 — Chart data
2 — Use of other instruments to fill in data, or large amount of radio or other interference subtracted	
	1 — Raw data, another instrument
	2 — Processed data
	3 — <a href="#">Corrected data</a>
6 — Interpolated data	
	9 — 95 to 99.9% of data present
	8 — 90 to 95% of data present
	7 — 85 to 90% of data present
	6 — 80 to 85% of data present
	5 — 70 to 80% of data present
	4 — 60 to 70% of data present
	3 — 50 to 60% of data present
	2 — 40 to 50% of data present
	1 — 30 to 40% of data present
	0 — less than 30% of data present
7 — Calculated data	
	1 — Diffuse
	2 — Tilted
9 — Missing or bad data	
	9 — Missing or bad data
0 — Chart data (obsolete)	
	9 — Chart data (obsolete)

### Notes

**Flag 13.** Data flagged 13 is not reliable for use in developing models. Often data is flagged 13 if it might have something wrong. For example, it's not always possible to discern the precise time when an Eppley NIP goes out of alignment. If the NIP is known to be out of alignment on a particular day, then the direct normal data for the previous day may be flagged 13.

**Flag 23.** Data are corrected only if we can be reasonably sure of the correction, and if the resulting values are within 5% of the actual values. For example, if snow is building up on a pyranometer during the first part of the day, and the direct beam measurements show that there were few—if—any clouds, it is sometimes possible to

correct the global values. Any values that are manually changed from the original data are flagged 23.

#### [SRML station ID codes](#)

The Solar Calculator relies on a 5-digit number in cell A1 of the active Excel worksheet to initially determine which station profile to load. For your own data files, we recommend that you avoid using any codes that have historically been associated with SRML stations. The following table lists most of these, though we add new ones from time to time. The table also provides a standard 2-character identifier for each station; we use these in naming our data files. Please note that some of the monitoring stations listed are not currently in service, and certain others are privately operated, requiring that special permission be obtained to use data gathered there.

ID code	Location	Abbrev
94002	Portland DEQ, OR	P1
94003	Milwaukie MES, OR	PL
94005	Gladstone, OR	GL
94007	Scoggins Creek, OR	SC
94008	Forest Grove, OR	FG
94019	Aprovecho, OR	AP
94040	Ashland, OR	AS
94101	Green River, WY	GR
94102	Moab, UT	MO
94145	Dillon, MT	DI
94158	Cheney, WA	CY
94166	Klamath Falls, OR	KF
94167	Whitehorse Ranch, OR	WH
94168	La Grande, OR	LG
94169	Hermiston, OR	HE
94169	Hermiston (AgriMet), OR	HN
94170	Burns, OR	BU
94171	Twin Falls (Kimberly), ID	TF
94171	Twin Falls (Agrimet), ID	TW
94172	Picabo, ID	PI
94173	Parma, ID	PA
94174	Aberdeen, ID	AB
94181	Coeur d'Alene, ID	CD
94182	Boise, ID	BO
94249	Silver Lake, OR	SL
94250	Klamath Falls, OR	KF
94251	Christmas Valley, OR	CH
94252	Madras, OR	MA
94253	Corvallis, OR	CV
94254	Willamette High School, Eugene, OR	WI
94255	Eugene, OR	EU
94256	Bend, OR	BE
94257	Coos Bay, OR	CB
94258	Portland, OR	PT
94277	Hood River, OR	HR
94278	West Hood River, OR	WR
94279	Parkdale, OR	PD



[Top of page](#)

© 2004, UO Solar Radiation Monitoring Laboratory.  
Last revised: January 21, 2004.  
Home page URL: [solardat.uoregon.edu](http://solardat.uoregon.edu)